

Role of Kerogen on the Solvent Retention and Sedimentation of Oil Sands in Non-Aqueous Bitumen Extraction

by

Farhad Azam

A thesis submitted in partial fulfillment of the requirements for the degree of

Master of Science

in

Materials Engineering

Department of Chemical and Materials Engineering
University of Alberta

© Farhad Azam, 2020

Abstract

One of the most problematic challenges of current hot water oil sands extraction methods is tailings ponds and the resulting environmental liability and risk. As a new method of extraction, non-aqueous extraction has the potential to replace the current hot-water extraction technology and eliminate the tailings ponds. Non-aqueous extraction can also substantially reduce the energy consumption for the extraction process, thereby reducing greenhouse gas emissions. Preliminary tests using solvents rich in cycloalkyl hydrocarbons, such as cyclohexane have confirmed that these solvents are capable to efficiently recover bitumen from the oil sands. Because non-aqueous bitumen extraction is not well known, characterizing inorganic and organic matter during a non-aqueous bitumen extraction process is a motivation for many researchers. Kerogen as an organic part of the oil sands is the subject of this research to understand its migration during extraction, and its effect on solvent retention and sedimentation of fine particles during non-aqueous extraction.

The novel particle fractioning in a water/cyclohexane mixture shows that particles containing kerogen are accumulated in the hydrophobic fraction and migrate to the cyclohexane portion. Mass spectrometry measurements show that an increase of kerogen from 1 wt% to 5 wt% in the oil sand end members elevates solvent retention at room temperature from 80 to 226 ppm. This residual solvent could be released at a higher temperature of 50°C. Sedimentation of oil sands with different kerogen and bitumen contents revealed that kerogen has a slight effect on fine particle sedimentation, which makes the total process of settling slower and fine particles tend to stay in the supernatant.

Acknowledgments

I would like to take this opportunity to express my genuine appreciation and gratitude to Dr. Thomas H. Etsell for his friendly manner and comprehensive support throughout this work. I am also grateful for Dr. Douglas G. Ivey's assistance with improving my thesis by his comments and corrections.

I would like to thank Dr. Mirjavad Geramian for his valuable inputs and comments during discussions and data analysis especially for his collaboration in semi-quantitative XRD calculations.

I would also like to thank Dr. Reza Sabbagh for developing the *MATLAB* code for linear regression employed in this research

My deepest thanks goes to my family for their love, support, and being a great encouragement in my life. Special thanks to my dearest, Zahra, for her endless love and kindness, energy, support and patience in my life including my current research.

Table of Contents

Abstract	ii
Acknowledgments.....	iii
Table of Contents	iv
List of Tables	vii
List of Figures	viii
List of Abbreviations	xii
1 Introduction	1
2 Literature review	4
2.1 Alberta oil sands	4
2.2 Bitumen extraction methods	6
2.2.1 Surface mining and hot water extraction.....	6
2.2.2 In-situ bitumen extraction.....	7
2.2.3 Non-aqueous bitumen extraction.....	8
2.3 Geology of Alberta’s oil sands	9
2.4 Mineralogy of oil sands	10
2.4.1 Inorganic matter in oil sands	10
2.4.2 Organic matter in oil sands.....	14
2.5 Summary.....	20

3	Experiments.....	22
3.1	Materials and material processing	22
3.1.1	Dean-Stark extraction	23
3.1.2	Kerogen extraction	23
3.2	Characterization methods.....	26
3.2.1	Random orientation X-ray diffraction	26
3.2.2	Organic elemental analysis.....	27
3.2.3	Scanning electron microscopy (SEM).....	27
3.2.4	Solvent retention analysis using QIC-MS	28
3.2.5	Particle size distribution analysis	28
3.2.6	Settling rate measurement	29
4	Results and discussion.....	31
4.1	Oil sands end members	31
4.2	Kerogen extraction and characterization	33
4.2.1	Homogenizing and Dean-Stark extraction	33
4.2.2	Bitumen free oil sands particle fractioning.....	34
4.2.3	Acid leaching of hydrophobic marine clay fraction	41
4.2.4	Extracted kerogen fractions analysis	44
4.3	Solvent retention by kerogen	49
4.3.1	Sample preparation	49

4.3.2	Drying time measurement	49
4.3.3	Sample preparation for solvent retention experiments	50
4.3.4	Calibration equation of QIC-MS response with cyclohexane	52
4.3.5	Cyclohexane desorption results	53
4.4	Effect of kerogen content on the particle sedimentation	55
4.4.1	Behavior of different fractions of MC-DS in different media.....	55
4.4.2	Effect of kerogen content on particle sedimentation	62
5	Conclusions and future work	68
5.1	Summary and conclusions	68
5.2	Future work.....	71
6	References	72

List of Tables

Table 1-1: Actual and forecast amounts of crude bitumen production in Alberta ($10^3 \text{ m}^3/\text{d}$) ¹	2
Table 4-1: Bitumen, water and solid contents of all end members from Syncrude’s North Mine and Aurora Mine.	32
Table 4-2: Total carbon content (TC) and Total organic carbon content (TOC) for all end members measured by CHNS before and after HCl treatment, respectively.	32
Table 4-3: Bitumen, water and solid contents in oil sands marine clay end member from Syncrude’s Aurora Mine.	33
Table 4-4: Average size distributions for MC-DS partitions in water/cyclohexane.	37
Table 4-5: EDX analysis results (wt%) after wet and dry hot leaching.	42
Table 4-6: CHNS elemental analysis of Aurora Mine marine clay bitumen and its different fractions of extracted kerogen.	45
Table 4-7: Mineral composition (wt%) of different fractions of Aurora Mine marine clay and kerogen determined by RockJock 11 software.	48
Table 4-8: Residual cyclohexane in MC-DS with different kerogen contents.	55
Table 4-9: Sedimentation rates of 1 st and 3 rd stages for MC-DS in water and cyclohexane. .	59
Table 4-10: Sedimentation rates of linear stages for MC with different bitumen and kerogen contents in cyclohexane.	67

List of Figures

Figure 1-1: Actual and forecast amounts of crude bitumen production in Alberta ¹	2
Figure 1-2: Total area of oil sands tailings ponds over time ⁷	3
Figure 2-1: Alberta’s oil sands areas ¹⁰	5
Figure 2-2: Typical arrangement of oil sands particles ¹¹	5
Figure 2-3: Hydrocarbon formation during sedimentation ⁶¹	15
Figure 2-4: Modified van Krevelen diagram for the Aurora Mine geological end members showing the position of end members on the plot between type II and III kerogen ⁶⁸	19
Figure 3-1: Flow diagram for the schematic experimental set-up for mineralogical and chemical composition characterization of four petrologic end members.	22
Figure 3-2: Schematic of Dean-Stark apparatus used in the study.	24
Figure 3-3: Flow diagram of kerogen extraction method and characterizing methods.	25
Figure 3-4: Flow diagram of sample preparation to measure solvent retention by QIC-MS and study sedimentation behavior by sedimentation balance.....	26
Figure 3-5: Schematic of sedimentation apparatus and resulting mass vs. time graph.	30
Figure 4-1: Bitumen content (wt%) in oil sands marine clay end member from Syncrude’s Aurora Mine.....	34
Figure 4-2: Water content (wt%) in oil sands marine clay end member from Syncrude’s Aurora Mine.....	34
Figure 4-3: Partitioning of MC-DS based on hydrophobicity. (a) In water, (b) in water/cyclohexane after 1 h, (c) in water/cyclohexane after 24 h.	35

Figure 4-4: Particle size distribution for marine clay after Dean-Stark (MC-DS) for different time periods.....	36
Figure 4-5: MC-DS particle size percentiles for different time periods.	36
Figure 4-6: Particle size distribution for hydrophilic (MC-L) and hydrophobic (MC-B) fractions of MC-DS.....	38
Figure 4-7: XRD patterns for random preparations of bulk samples of MC-DS and MC-B. I, illite; K, kaolinite; Q, quartz; D, dolomite; M, magnetite.....	39
Figure 4-8: Total carbon content of marine clay samples measured by CHNS before HCl treatment.	40
Figure 4-9: Total organic carbon content of marine clay samples measured by CHNS after HCl treatment.	40
Figure 4-10: XRD patterns for random preparations of bulk samples of MC-B and MC-HCl. I, illite; K, kaolinite; Q, quartz; D, dolomite; M, magnetite.....	41
Figure 4-11: EDX mapping for MC samples after acid treatment by HCl-HF. (a) wet condition and (b) dry condition.....	43
Figure 4-12: XRD patterns for random preparations of bulk samples of different fractions of kerogen extracted from Aurora Mine marine clay. Ral, ralstonite; Ros, rosenbergite; Mag, magnetite; Ch, Chromatite; An, annite; Py, pyrite; Q, quartz.....	47
Figure 4-13: Secondary electron image of SEM and EDX analysis of the newly formed fluorides after HCl-HF treatment of marine clay.....	48
Figure 4-14: Total weight loss of MC-DS sample saturated with MC-DS:cyclohexane ratio of 60:40.	50
Figure 4-15: QIC-MS results for desorbed gases from MC-DS mixed with cyclohexane.	51

Figure 4-16: Calibration plot of QIC-MS response for known volumes of cyclohexane.....	52
Figure 4-17: Average responses of QIC-MS for samples with different kerogen contents. ..	53
Figure 4-18: Elapsed time for cyclohexane desorption from MC-DS with different amounts of kerogen.....	55
Figure 4-19: position of the probe in sedimentation balance.....	56
Figure 4-20: MC-DS after 30 min sedimentation. (a) In water, (b) in cyclohexane.....	57
Figure 4-21: Sedimentation behavior of MC-DS in water and cyclohexane, measured by a sedimentation balance. (a) Sedimentation in full scale, (b) closer view of stage one, (c) closer view of stage three.	59
Figure 4-22: Sedimentation behavior of MC-DS and its fractions, MC-B and MC-L, in water, showing the effect of particle characteristics on the 1 st and 3 rd stages of sedimentation as reflected in the graph slope equations. (a) Sedimentation in full scale, (b) closer view of stage one, (c) closer view of stage three.	60
Figure 4-23: Sedimentation of MC-DS in different media, showing the effect of media on the 1 st and 3 rd stages of sedimentation as reflected in the graph slope equations. (a) Sedimentation in full scale, (b) closer view of stage one, (c) closer view of stage three.	61
Figure 4-24: Sedimentation behavior of MC with different bitumen contents in cyclohexane, showing the effect of bitumen content on the 1 st and 3 rd stages of sedimentation as reflected in the graph slope equations.....	63
Figure 4-25: Sedimentation of MC-5 wt% bitumen without kerogen and with 3 and 5wt% kerogen in cyclohexane. (a) Sedimentation in full scale, (b) closer view of stage one, (c) closer view of stage three.	64

Figure 4-26: Sedimentation of MC-10 wt% bitumen without kerogen and with 3 and 5wt% kerogen in cyclohexane. (a) Sedimentation in full scale, (b) closer view of stage one, (c) closer view of stage three. 65

Figure 4-27: Sedimentation of MC-15 wt% bitumen without kerogen and with 3 and 5wt% kerogen in cyclohexane. (a) Sedimentation in full scale, (b) closer view of stage one, (c) closer view of stage three. 66

List of Abbreviations

MC: Marine Clay end member of oil sands

MS: Marine Sand end member of oil sands

EC: Estuarine Clay end member of oil sands

ES: Estuarine Sand end member of oil sands

MC-DS: Bitumen-free Marine clay after Dean-Stark oil extraction by Toluene

MC-L: Hydrophilic fraction of MC-DS after water/cyclohexane fractioning

MC-B: Hydrophobic fraction of MC-DS after water/cyclohexane fractioning

MC-xB: Constructed sample of MC-DS with x wt% bitumen added ($x = 5, 10, 15$)

MC-xB-yK: Constructed sample of MC-DS with x wt% bitumen and y wt% kerogen added ($x = 5, 10, 15$ and $y = 3, 5$)

K-top: The most pure extracted kerogen collected from top 2/3 of the extraction container

K-low: The extracted kerogen collected from remaining lower 1/3 of the extraction container

Heavy sediment: Residual mineral particles after kerogen extraction

SEM: Scanning Electron Microscopy

EDX: Energy-Dispersive X-ray spectroscopy

CHNS: Elemental analysis of Carbon, Hydrogen, Nitrogen and Sulfur

QIC-MS: Quartz Inert Capillary Mass Spectrometer

TC: Total Carbon content

TOC: Total Organic Carbon content

TN: Total Nitrogen content

1 Introduction

Total crude bitumen production in Alberta, reported by Alberta Energy Regulator, has reached the amount of 492'300 cubic meters per day or almost 3.1 million barrels per day by the end of 2019; almost half of this amount is recovered by surface mining as indicated in Table 1-1 and Figure 1-1^{1,2}. The efficiency of conventional extraction methods is influenced by the ore mineralogy and the chemistry of water and bitumen³⁻⁵. The Alberta oil sands are mixtures of different geological end members; estuarine and marine ores are the major ones. In each geological interval, claystone and oil sands are interbedded in each other, such that Alberta oil sands contain four petrologically different types of rocks called 'petrologic end members' (marine clay, marine sand, estuarine clay and estuarine sand). The mined oil sands are different combinations of these four petrologic endmembers, so their properties in various mining sites and the recovery of bitumen may be attributed to a combination of the properties of these different end members. The conventional water extraction methods for oil sands consume a lot of water and produce large amounts of tailings. By the end of 2016, tailings ponds and their operating structures like dikes occupied about 257 square km of northern Alberta lands; 103 square km of this amount was the liquid surface area of the ponds⁶⁻⁸. These tailing ponds areas are increasing rapidly with higher rates of bitumen production, that are planned to reach more than 4 million barrels per day by 2029^{1,2}. Figure 1-2 Shows the increasing rate of tailing ponds area in Alberta from 1985 to 2016⁷.

Figure S3.1 Alberta crude bitumen production

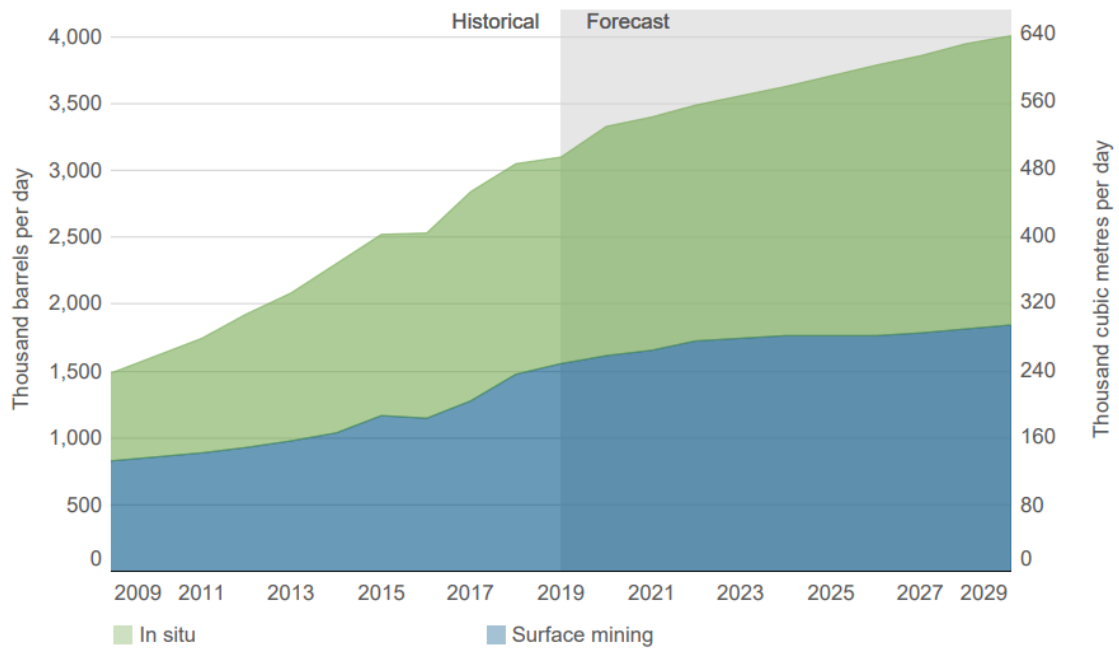


Figure 1-1: Actual and forecast amounts of crude bitumen production in Alberta ¹.

Table 1-1: Actual and forecast amounts of crude bitumen production in Alberta (10³ m³/ d) ¹.

Raw production	2018	2019	2020	2021	2029
Mineable	234.1	246.5	256.4	263.4	293.1
In situ	250.4	245.8	272.8	277.5	343.8
Total	484.5	492.3	529.2	540.9	636.9

To reduce the environmental impact of bitumen extraction, non-aqueous solvent bitumen extraction has been investigated. These methods reduce water consumption and tailings production, which are the main drawbacks of conventional water-based bitumen extraction.

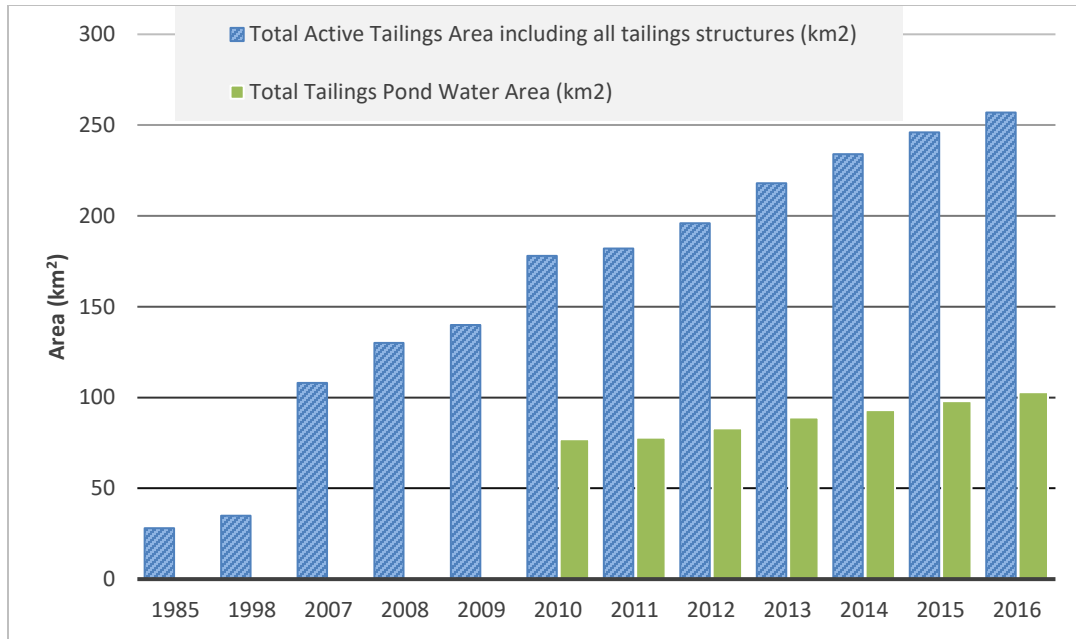


Figure 1-2: Total area of oil sands tailings ponds over time ⁷.

As mentioned, ore mineralogy or oil sands composition is one of the main parameters affecting bitumen extraction. Therefore, mineral and chemical characterization of the end members is essential for better understanding of the mineralogical and geochemical factors affecting aqueous or non-aqueous bitumen extraction and solvent recovery from the extraction tailings. Many researchers studied the effect of different parts of oil sands, including inorganic and organic parts, on oil sand extraction process.

Kerogen as an organic part of oil sands affects the oil sand extraction process by varying the amount of solvent retention in the tailing and also the behavior of fine particles and their sedimentation performance. Thus, it is important to study the effect of kerogen on the oil sand extraction process. The goal of this research is to address the lack of information about kerogen behavior in non-aqueous oil sands extraction. This includes the study of kerogen migration during non-aqueous extraction, and its effect on solvent retention and sedimentation of fine particles.

2 Literature review

2.1 Alberta oil sands

Providing thousands of jobs and millions of dollars of royalties to the government, oil is a major industry in Alberta. In terms of proven global crude oil reserves, Alberta ranks third, after Saudi Arabia and Venezuela. Alberta's total established oil reserves are about 176.8 billion barrels, or about 11 percent of total global oil reserves^{1,2,9}. As illustrated in Figure 2-1, oil sands in Alberta cover 140,200 square kilometers in three regions of northern Alberta: Athabasca, Peace River and Cold Lake¹⁰. Oil sands are a complex mixture of bitumen, inorganic materials and salty water, including 55–80 wt% inorganic materials, 4–18 wt% bitumen and 2–15 wt% water^{3,11-13}. The generally accepted arrangement of oil sands components is illustrated in Figure 2-2¹¹. These deposits are a combination of organic matter and inorganic sediments, affected by sufficient pressure and temperature over thousands of years to be altered into oil and sandstone. Sedimentation happened in two main sedimentary surroundings, marine and estuarine, which created four types of 'petrologic end members' including estuarine sand, estuarine clay, marine sand and marine clay. This structure makes recovery of oil from oil sands a considerably challenging prospect. Also the extracted bitumen has a higher density and viscosity compared to conventional crude oil, due to the presence of high molecular weight organic matter¹⁴. A diverse mixture of these end members is present in any oil sands deposit mined in Alberta, affecting the bitumen extraction procedures.



Figure 2-1: Alberta's oil sands areas ¹⁰.

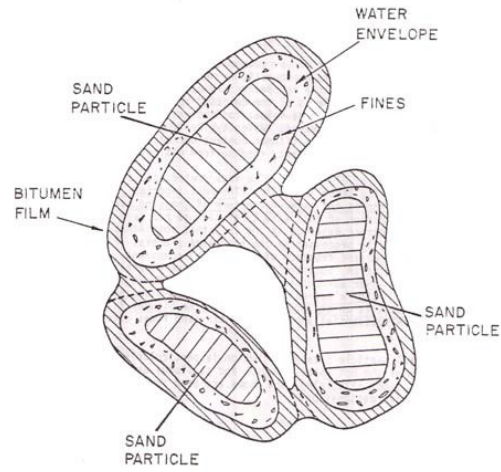


Figure 2-2: Typical arrangement of oil sands particles ¹¹.

2.2 Bitumen extraction methods

According to the depth of deposits, the Alberta oil sands are divided in two categories; shallow deposits found to a depth of 75 m or less, and deep deposits beyond this threshold. Conventional extraction methods using open-pit mining followed by hot water extraction processes are used for shallow deposits to produce 45% of the total extracted bitumen in Alberta^{1,2}. In-situ extraction techniques including steam assisted gravity drainage (SAGD) and vapor extraction (VAPEX) are utilized for deeper deposits¹⁴.

2.2.1 Surface mining and hot water extraction

Commercially, water-based extraction that is used to extract bitumen from oil sands consists of three fundamental steps: liberation (separation) of bitumen from sand grains; aeration (attachment or engulfment) of the liberated bitumen to air bubbles; and flotation of bitumen–air bubble aggregates to the top of the slurry to form a bitumen-rich froth¹⁵. In the hot water extraction process, bitumen is effectively removed by froth flotation by creating a slurry via mixing water at 80°C and a pH of approximately 8.5 with the ore¹⁶. More recently, the hot water process has been modified to a warm water hydro-transport process, where the ore is conditioned in a pipeline with warm water (45°C to 55°C) at a pH between 7 and 8.5 prior to froth separation. Bitumen liberation and aeration are controlled by interactions among bitumen, solids, water and air, which are influenced by many factors like the process temperature, mechanical agitation, water chemistry (controlled by chemical additives), bitumen chemistry and the mineralogy of the ore and its interfacial properties¹⁷⁻¹⁹. This extraction process is very water-intensive; to produce each barrel of oil from oil sands, 2.6 m³ of water and 2 tons of ore are used which creates

about 0.50 m³ of mature fine tailings or MFT^{12,13}. This MFT is a mixture of water, residual organics (bitumen, tightly bound organics and solvents) and fines (<45µm size fraction). By 2016, 257 square kilometers of land in northern Alberta are covered by oil sands tailings; the area is increasing everyday due to an increasing rate of bitumen production. The close proximity of the tailings ponds to the Athabasca River requires that the ponds be monitored and maintained for decades after mine closure to prevent discharge into the river. A potential environmental liability would be a consequence of this rapid increase of tailings. Therefore, applying organic solvents for bitumen extraction (non-aqueous extraction) from the oil sands is an alternative to the current commercial water based extraction process.

2.2.2 In-situ bitumen extraction

For deeper bitumen deposits, in-situ extraction methods have been developed like SAGD and VAPEX. In the SAGD process, steam is injected into a horizontal well and the temperature is increased, which leads to viscosity reduction of the bitumen. This low viscous bitumen is drained to the surface by another horizontal well, drilled parallel to the steam injection well five meters below¹⁴. VAPEX is a newer technique using a solvent vapor to dilute bitumen and decrease its viscosity. Similar to SAGD, a solvent vapor is injected via an upper horizontal well and diluted bitumen flows to the lower horizontal well under gravity and finally drains out to the surface. These methods are not only energy intensive, but also produce greenhouse gases leading to environmental concerns.

All the above issues, including the high amount of water consumption which leads to a rapid increase in the area covered by tailing ponds and its environmental concerns, as well as the large energy intake which increases greenhouse gas emission, necessitate exploration of new methods of bitumen extraction.

2.2.3 Non-aqueous bitumen extraction

Non-aqueous bitumen extraction is an interesting area of study to develop more economical and environmentally friendly methods of bitumen extraction, which use lower amounts of water, use less energy to extract bitumen from oil sands and generate dry tailings that eliminate the problem of tailing ponds.

Different light hydrocarbon solvents were studied for bitumen extraction at room temperature and pressure by Nikakhtari et al. ²⁰. They pointed out that among all tested aromatics, cycloalkanes and biologically derived solvents, cyclohexane has higher bitumen recovery and lower residual content in the remaining oil sands tailings. They suggested cyclohexane as the best and isoprene as the second best suitable solvents for bitumen extraction ²⁰. In another study by Hooshiar et al. ²¹, two oil sands samples with different fines and clay contents were treated by non-aqueous solvent extraction using different ratios of toluene and heptane. This study showed that, contrary to the water extraction process, fines and clay contents do not influence the bitumen recovery from oil sands. To understand clay particle behavior during solvent extraction, Hooshiar et al. characterized these two oil sands, their supernatant and tailings from the same solvent extraction

procedure. This study revealed that, in both samples, kaolinite and illite were the main clay minerals, and kaolinite was enriched in the supernatant ²².

2.3 Geology of Alberta's oil sands

The Alberta oil sands are mixtures of different geological end members. The major geological members mined at the Syncrude site are estuarine and marine ores, for which in each geological interval, claystone and oil sands are interbedded in each other. Thus, Alberta oil sands contain four petrologically different types of rocks called 'petrologic end members' (marine clay, marine sand, estuarine clay and estuarine sand), deposited in marine and estuarine sedimentary environments and mined oil sands are different combinations of these four petrologic end members.

Estuarine ore is usually the main production interval due to the shallowness of the marine ore interval. In estuarine ore, the claystone is pale and grey in color and thus distinguishable from the estuarine sand, layer by layer. However, although marine sand and clay are interbedded like estuarine ore, marine clay is as black and dark as marine sand. As mentioned, the mined oil sands are different combinations of these four petrologic end members, so the recovery of bitumen using non-aqueous extraction may be attributed to a combination of the properties of these different geological end members. The differences among oil sands ores are due to various mineralogy and organic petrology, in which clays and kerogen are the most important indicators.

The residual organic matter (bitumen and solvents) in the tailings is an accompanying problem with bitumen extraction. Any loss in bitumen recovery results in the existence of

residual bitumen in the tailings, so higher bitumen recovery is not only important economically but is also advantageous environmentally. Also, due to the large scale of oil sands production, a minor improvement in bitumen recovery has a major economic impact. Therefore, understanding the influence of oil sands mineralogy on any oil extraction processes is highly essential.

2.4 Mineralogy of oil sands

Oil sands are combinations of organic and inorganic components. The inorganic part consists of mainly sands and clays, while the organic part includes mostly heavy bitumen and insoluble organics, known as kerogen.

2.4.1 Inorganic matter in oil sands

Quartz is usually the major non-clay mineral, while kaolinite, illite, chlorite, smectite and interstratified clay minerals are the main clay minerals in Alberta oil sands. Other non-clay minerals are predominantly carbonates, K-feldspar and TiO₂ minerals²³⁻²⁸. Among clay minerals, kaolinite and illite are present as major clay minerals in Athabasca oil sands, while minor amounts of chlorite, discrete smectite and mixed-layer clay minerals are also observed²⁹⁻³². Almost all these inorganic components can be divided in two categories of clay minerals and non-clay minerals.

2.4.1.1 Non-clay minerals

The most common sand component in Alberta oil sands is quartz with 70 – 90 wt% occurrence³³. However, in the Earth's crust, feldspar minerals are dominant at almost 60% and quartz is the second most abundant mineral. In Alberta oil sands after quartz, K-, Na- and Ca-feldspars are the most common minerals^{12,33,34}. These sands are usually in the size range of 45 µm and larger and are believed to cause no problems throughout the extraction process^{3,12,35-37}. Yet, some quantities of quartz, feldspar and Ti-, Zr- and Fe-bearing minerals have been observed in the <45 µm fraction and are carried forward into the bitumen froth due to the presence of some fine particle sizes as well as being attached to other fine clay particles or hydrophobic toluene insoluble organic matter^{12,27,36,38}.

Carbonates are the other non-clay minerals in the oil sands. Carbonate rocks hold several massive conventional reservoirs in Saudi Arabia and Iraq, as well as more than half of the conventional crude oil in Alberta. Also, some giant bitumen reservoirs in north central Alberta are carbonate, such as the Devonian Grosmont platform, which has the largest carbonate bitumen reservoir at depths of 250-400 m⁴⁰⁻⁴³. Siderite (FeCO₃) and its isomorph calcite (CaCO₃), as well as dolomite (CaMg(CO₃)₂) and its isomorph ankerite (Ca(Mg,Fe)(CO₃)₂), are four abundant carbonates present in Alberta oil sands^{12,44-46}. Hydrophobicity properties of siderite are more pronounced than other non-clay minerals⁴⁷, which can justify its presence in the primary froth, as well as being detected in all fractions of the ore, especially in the coarse fraction (>45 µm), as well as the tailings¹².

Other iron-bearing minerals and titanium-bearing minerals represent other non-clay minerals found in Alberta oil sands. The majority of these minerals accumulate in the <45 µm fraction⁴. These fine particles migrate predominantly to the primary froth and fine

fractions^{12,27}. The total quantity of Ti-bearing minerals in the McMurray Formation is reported to be between 0.05 and 0.40 wt%, while their amount is elevated to 4-15 wt% in the bitumen free froth solids⁴⁸.

2.4.1.2 Clay minerals

Clay minerals, identified in the Alberta oil sands deposits, are the most likely minerals that contribute to unexpected behavior during bitumen extraction. These minerals, collectively called ‘clays’, are susceptible to interaction with the solvent, bitumen and/or water due to their high specific surface areas, high cation exchange capacities or redox activities, layer charges and specific physicochemical properties. Clay minerals have layered crystal structures with varying chemical composition, varying physical properties and particle size smaller than 2 μm . The layers of clay structures are tetrahedral and octahedral sheets stacked on top of each other. Clay minerals can be categorized based on the order of this stacking sequence. The two main layering types of clays are the 1:1 (tetrahedral:octahedral) sheets and the 2:1 (tetrahedral:octahedral:tetrahedral) sheets. Of these structures, 2:1 stacking is most likely to have negative layer charges and others are neutral or slightly charged on the layers⁴⁹. The charges are due to ionic substitution in the layers; ionic substitutions of Al^{+3} for Si^{+4} in the tetrahedral sheets and Fe^{+2} and Mg^{+2} for Al^{+3} in the octahedral sheets are the main sources of negative charges in clays like smectite. In addition, the surface of clays can be temporarily charged differently in different pHs. In the layered structure, unit layers are bonded together firmly by hydrogen bonds while the units themselves are not strongly bonded and create cleavage planes. The layer thickness of 1:1 clays are in range of 0.7 nm, while for 2:1 the thickness depends on the interlayer

composition and can vary from 0.91 nm to 1.5 nm⁵⁰. This layer structure allows water molecules to be absorbed in the interlayer spaces as well as adsorbed on the external surfaces and edges⁴⁹. In some clays, like smectite and kaolinite, the absorbed water in the interlayer spaces causes expansion of the clay structure and swelling of the clay, which results in gel formation after water absorption^{50,51}.

Bitumen molecules are exposed to the highly reactive clay minerals during the extraction process, which leads to an irreversible adsorption of organic matter (e.g., bitumen or bitumen components such as asphaltenes) on clay mineral surfaces. This adsorption of bitumen on clay alters the physical and chemical properties of the clay minerals as well as the crude oil composition. Both of these changes influence the extraction process^{52,53}. Thus, by increasing the clay content of an ore, the bitumen recovery decreases, which is a general trend regarding the effects of mineralogy on extraction that has been observed over the years.

It has also been shown that the addition of montmorillonite and calcium ions has a synergistic effect in decreasing bitumen recovery, whereas the addition of other clay minerals (kaolinite and illite) does not have such an impact on recovery. The relationship between increased soluble potassium and decreased bitumen recovery has been studied and shows degraded illite has a negative impact on recovery⁵⁴. The relationship between several characteristics of clay minerals in the oil sands ores and bitumen recovery has been studied by x-ray diffraction (XRD), which indicates there is a correlation between bitumen recovery and the ratio of illite to kaolinite in the raw oil sands ore³⁰. Another study showed that the ultrafine (<0.3 µm) clays may be responsible for gelation and the sludging behavior of some ores, which negatively affects bitumen recovery and tailings management⁵⁵. In

other words, increased surface area (decreased particle size), an increase in surface charge (i.e., degraded illite/smectite) and an asymmetric particle shape all make bitumen flotation more difficult due to an increase in the yield strength of a slurry of particles^{12,56}. These studies emphasize the importance of clay characterization in the oil sands, as they all indicate that the presence of clay in oil sands causes poor recovery of bitumen.

In the oil sands industry where hot water extraction process is used, it is generally recognized that bitumen recovery decreases with increasing fines (<45 µm) content in the oil sands^{57,58} and, in particular, that the clay mineral component is important (size fractions <3 µm)^{30,55,59,60}. Also, the negative effects of clay minerals on bitumen extraction from the oil sands have been reported^{31,54,59,60}. In addition, it has also been proposed that the presence of Fe (oxyhydr)oxides with high surface area may have negative consequences on bitumen extractability from the oil sands³¹. Hence, mineral and chemical characterization of the four petrologic end members are crucial for better understanding of the mineralogical and geochemical factors affecting aqueous or non-aqueous bitumen extraction and solvent recovery from the extraction tailings.

2.4.2 Organic matter in oil sands

Organic matter including petroleum, bitumen, coal, natural gas and kerogen are produced from alteration of living organism debris stuck between sediments over thousands of years. Through this burial period, most of these organisms are decomposed and cracked to smaller molecules and recycled, but some are preserved in the shape of higher molecular weight organic matter. Two paths of geochemical fossil and kerogen

degradation are the most important sources of hydrocarbon formation during sedimentation. These are shown schematically in Figure 2-3 ⁶¹.

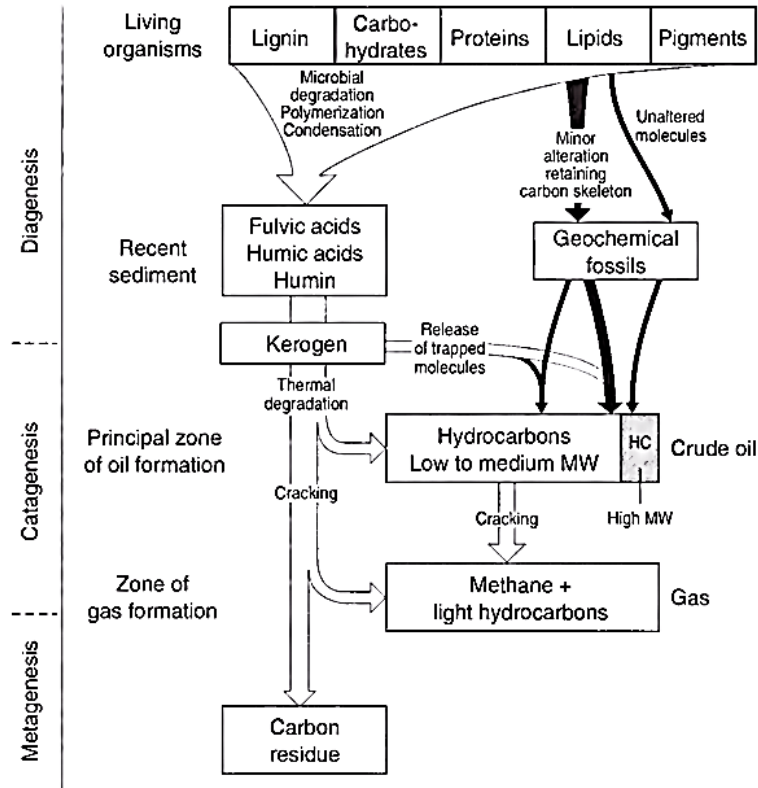


Figure 2-3: Hydrocarbon formation during sedimentation ⁶¹.

Based on different combinations of temperature, pressure and time, diagenesis, catagenesis and metagenesis will occur that transform buried living debris to hydrocarbons. Near the surface, low temperatures (up to 60°C) and pressure dominate and diagenesis occurs producing methane, carbon dioxide, kerogen and water. By increasing the depth of burial and, consequently, higher temperatures (60-175°C) and pressure, catagenesis transforms kerogen to liquid hydrocarbons. At still higher temperatures, kerogen and bitumen are altered to methane and light hydrocarbons through the metagenesis process ⁶².

Along with bitumen, which is the desired organic matter in oil sands and the target of extraction, kerogen is another organic matter, which is found in Alberta oil sands.

2.4.2.1 Bitumen

Bitumen is an extremely viscous liquid that, contrary to conventional crude oil, cannot flow at room temperature. To make it flow, it should be either heated or diluted. Bitumen is a mixture of heavy hydrocarbons, with higher carbon to hydrogen ratio than conventional crude oil. Also, high amounts of impurities including nitrogen, sulfur and heavy metals are embedded in bitumen, which need to be eliminated prior to almost any use. Bitumen is a complex mixture of different organic molecules with a vast range of molecular weights from methane to molecular weight molecules larger than 15,000 Da. Characterization of bitumen in Alberta oil sands has revealed various structures (paraffinic, aromatic, olefinic, and heterocyclic) with many different functional groups ⁶². In general, bitumen is divided into four main components including saturates, aromatics, resins and asphaltenes, known as SARA. Different solvents are able to dissolve desired components. Generally, by increasing the molecular weight of the components, solubility decreases. Aromatic and polar solvents like benzene or toluene can dissolve all components, but paraffinic solvents are not able to dissolve resins and asphaltenes ⁶³. In Alberta oil sands, along with bitumen, a remarkable quantity of kerogen is also present that is considered as non-soluble organic matter.

2.4.2.2 Kerogen

The word kerogen invented in early 1910s by Crum-Brown during a study on the organic matter of a Scottish oil shale. Through the distillation of this oil shale a waxy oil was produced that inspires creating the word kerogen to describe this organic matter. Keros means wax and kerogen is an organic matter with the capability to generate oil. This organic matter is tightly mixed with minerals and insoluble in solvents. Forsman investigates its isolation methods from 1960s. Kerogen is a generic name, like lipids or proteins, and cannot be represented with a chemical composition. Different mixtures of organic precursors produced wide range of kerogen structures and diverse geological burial conditions including time, temperature and pressure may change kerogen composition and structure. Kerogen is a precursor of oil and gas and during this condition, a part of it transformed to petroleum and gas ^{64,65}.

At the beginning of sedimentation, kerogen forms at mild temperatures and pressures from lipids or lignin present in animal tissue and plant matter. More sedimentation increases burial depth and, consequently, kerogen is exposed to higher pressure and temperature which leads to rearrangement of its structure and generation of hydrocarbons, such as oil, gas and bitumen⁶⁶. Kerogen changes during burial and the amounts of hydrogen and oxygen in its structure decrease. The different hydrogen, carbon and oxygen ratios are used to classify kerogen ⁶⁷.

Rock-Eval is a fast and precious characterization method to determine the source rock type, already present hydrocarbons and remaining hydrocarbon potential in the sample. This pyrolysis-based method determines kerogen properties without any isolation or concentration from minerals. During a programmed heating, pyrolysis happens and an inert gas flow carries the generated effluents to a flame ionization detector. The free oil already

in the will be vaporized by heating to 300°C to form S1 peak, whereas heating in the range of 300-550°C release hydrocarbon due to thermal cracking of kerogen in the rock to create S2 peak. Infrared (IR) spectroscopy during the pyrolysis results peak S3 contributing to CO and CO₂ content of the sample ^{64,68}.

The basis of kerogen isolation is to destruct its accompanying minerals from finely ground sediment, using non-oxidant acids at low temperatures (< 60 °C). Hydrochloric acid (HCl) is to dissolve carbonates, sulfides, sulfates and hydroxides, then hydrofluoric acid (HF) to eliminate quartz and silicates. There are also two types of accompanying minerals with the extracted kerogen at the end; one would be minerals such as pyrite that resist against these acid attacks, and the other is newly formed complex fluorides such as ralstonite (Na_xMg_xAl_{2-x}(F,OH)₆H₂O) that are produces during the hydrofluoric acid treatment. Pyrite is a normal byproduct of bacterial kerogen formation and regularly covered by kerogen network. Due to this formation pyrite is not completely exposed to acid attacks and would be survived throughout the kerogen isolation procedures. Newly formed fluorides are prevented to a good extent by coupling HCl to HF (1/3 HCl and 2/3 HF v/v) at the second step of acid treatment ^{64,65}.

By combining Rock-Eval parameters and total organic carbon (TOC) analysis of samples, modified van Krevelen diagram will be plotted which shows the type and maturity of kerogen. The Modified van Krevelen diagram plots atomic hydrogen index (HI) versus oxygen index (OI). Hydrogen index (HI) is equal to (S2/TOC) ×100 representing mg hydrocarbon per g TOC and oxygen index (OI) is equal to (S3/TOC) ×100 expressing mg of CO₂ per g TOC ⁶⁸.

Type I kerogen is rich in hydrogen and low in oxygen and prone to produce oil. Type II kerogen is also high in hydrogen, but has lower oxygen and carbon contents. It is prone

to both oil and gas production. Type III has lower hydrogen and higher oxygen compared with types I and II and mostly releases gas with heating and maturation. Type IV has high carbon and low hydrogen content which has no potential for hydrocarbon production^{65,69,70}. It has been reported that 1% to 4% kerogen is present in Alberta oil sands; the type of kerogen is between type II kerogen (more in marine samples) and type III kerogen (more in estuarine samples)⁶⁸.

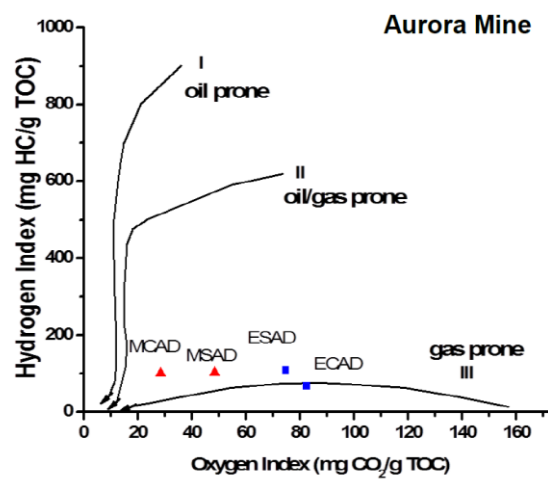


Figure 2-4: Modified van Krevelen diagram for the Aurora Mine geological end members showing the position of end members on the plot between type II and III kerogen⁶⁸.

Adsorption of chemical compounds like organic solvents, proposed to be used in non-aqueous extraction, onto kerogen is of importance. This adsorption of solvents to kerogen may lead to solvent retention in the gangue, which causes higher extraction costs and also brings environmental issues. Sorption of organic chemicals to soils and sediments is affected by adsorption to carbonaceous materials such as coal and kerogen. This adsorption is nonlinear and has a greater impact on total sorption of organic chemicals to soil and sediments, especially in low aqueous concentrations⁷¹.

2.5 Summary

As briefly discussed, the adsorption of organic matter (e.g., bitumen components, such as asphaltenes) on the clay mineral surfaces has a huge influence on the bitumen extraction process and also dramatically changes the physical and chemical properties of the clay minerals. Therefore, one has to be very careful when using general knowledge about the characteristics of the clay minerals present in the oil sands (kaolinite, illite, smectite and chlorite). For this reason, characterizing the clay minerals in a natural system (during actual bitumen extraction) is of great importance.

As a new method of extraction, non-aqueous extraction has the potential to replace the current hot-water extraction technology. Preliminary tests using solvents rich in cycloalkyl hydrocarbon solvents such as cyclohexane have confirmed that these solvents are capable of efficiently recovering bitumen from the oil sands. Successful application of this technology would eliminate the tailings ponds and the resulting environmental liability and risk and also substantially lower the energy consumption for the extraction process, thereby reducing greenhouse gas emissions. Because non-aqueous bitumen extraction is not well understood, conducting research to characterize clay minerals, non-clay minerals and insoluble organic matter during an actual non-aqueous bitumen extraction process is essential and a motivation for further research. Also, solvent retention by each component of the oil sands would be important as it has both economic and environmental impacts.

To address some of these questions, this research is planned to study the effect of kerogen as an organic part of oil sands in solvent retention of the oil sands tailings after the non-aqueous solvent extraction process. Cyclohexane, as a successful candidate solvent for non-aqueous oil sands extraction was chosen to extract the oil. The amount of remaining

solvent in the tailings was measured by utilizing a Quartz Inert Capillary Mass Spectrometer (QIC-MS). Also, to understand the effect of kerogen content in the oil sands on sedimentation behavior of fine particles during solvent extraction process, sedimentation of oil sands in cyclohexane is designed to be executed in a sedimentation balance.

3 Experiments

3.1 Materials and material processing

Oil sands ores from the North Mine and Aurora Mine of Syncrude Canada, Ltd. (Fort McMurray, Alberta) were used in this research. The oil sands ores, designated as MC (marine clay), MS (marine sand), EC (estuarine clay) and ES (estuarine sand), represent the four petrologic end members of estuarine and marine origin. The as-received petrologic end members were manually homogenized, disaggregated and passed through a sieve with an aperture size of 6.35 mm, then stored frozen in sealed containers before use. Bitumen, solids and water contents of bulk petrologic end members were determined by the Dean-Stark extraction method. The resulting bitumen free solids were dried at 60°C for 24 hours and ground gently to disaggregate the possible lumps. All bitumen free samples including the original four petrologic end members and the resulting solids after each step of processing were characterized by X-ray diffraction (XRD), elemental analysis, scanning electron microscopy (SEM) and energy-dispersive X-ray spectroscopy (EDX). Figure 3-1 shows a flow diagram of solid processing for characterization.

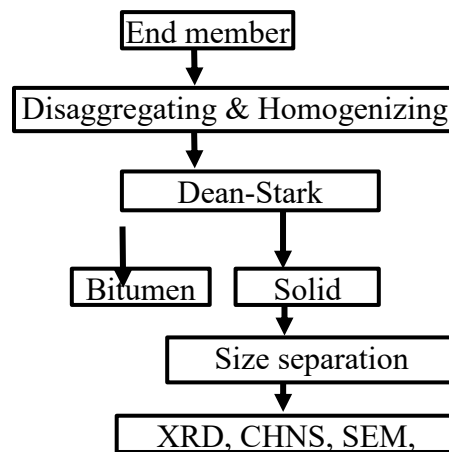


Figure 3-1: Flow diagram for the schematic experimental set-up for mineralogical and chemical composition characterization of four petrologic end members.

3.1.1 Dean-Stark extraction

To obtain bitumen free solids from oil sands end members, Dean-Stark extraction was used, which also provides the water and bitumen contents of oil sands end members. For this purpose, a well-developed setup was utilized which, includes a round-bottom flask that is placed on a hot plate and connected to a condenser to avoid any solvent vapor loss; the condenser is also equipped with a graduated trap to collect the water content of the oil sands. A thimble filled with oil sands hangs in the neck of the round-bottom flask. Then the flask is filled with toluene and placed on a hot plate to warm the toluene, which produces toluene vapor going up through the round-bottom flask neck and condenser. Cold water runs through the condenser to condense toluene and water vapors produced in the process. The oil sands in the thimble are in steady contact with the condensed toluene refluxing from the condenser, which dissolves bitumen and collects it in the flask. This process runs for 12 h to ensure all bitumen is dissolved and what remains in the thimble is the bitumen free oil sands solids. A schematic of this setup is illustrated in Figure 3-2.

3.1.2 Kerogen extraction

In order to characterize mineral associated kerogen, study the behavior of kerogen particles during non-aqueous bitumen extraction and evaluate the effect of kerogen on solvent retention, kerogen needs to be isolated from the end members. To obtain kerogen, the oil sands end member MC was prepared by grinding to pass a 6 mesh sieve with aperture size of 3.35 mm, and then Dean-Stark extraction was used for 12 h to remove all the bitumen in the samples. The bitumen-free marine clay (MC-DS) samples were subjected to water/cyclohexane fractioning to separate the kerogen containing fraction

based on the hydrophobicity. The kerogen containing particles accumulate in the hydrophobic fraction, which will float to the surface of cyclohexane. The hydrophobic fraction was separated by suctioning from the surface, while a clear distinguished mud line was observed between the water and cyclohexane portions. Hydrophilic particles settle down into the water and were separated for further characterization by XRD. The kerogen rich fraction was treated with concentrated HCl for three hours. The samples were then rinsed 10 times to remove any dissolved Ca ions. The residues from the HCl treatment were subsequently treated with 45% HF and agitated for two days. Fresh HF was added to the slurry on the second day. The leached residues were rinsed with deionized water to neutral pH (pH=7), followed by the addition of a small amount of HCl to dissolve any fluorosilicates. The resulting solid residues would be kerogen, which had been rinsed with deionized water to neutral pH. The kerogen extraction process is presented schematically in Figure 3-3.

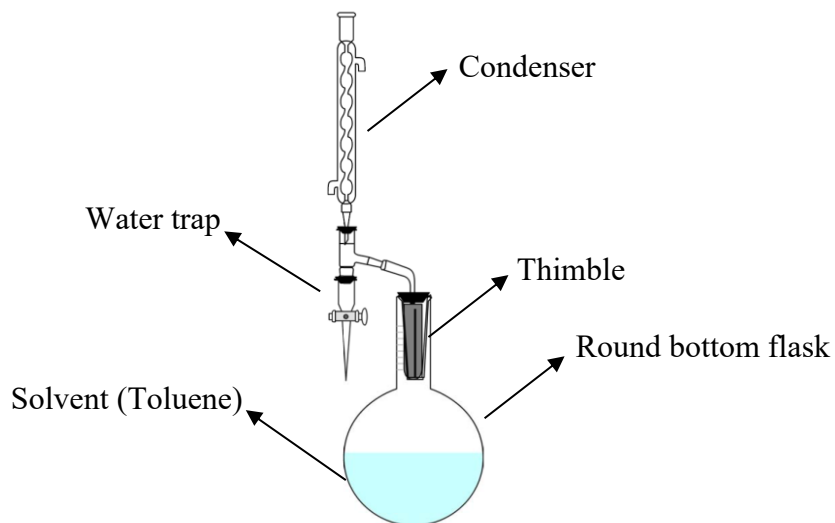


Figure 3-2: Schematic of Dean-Stark apparatus used in the study.

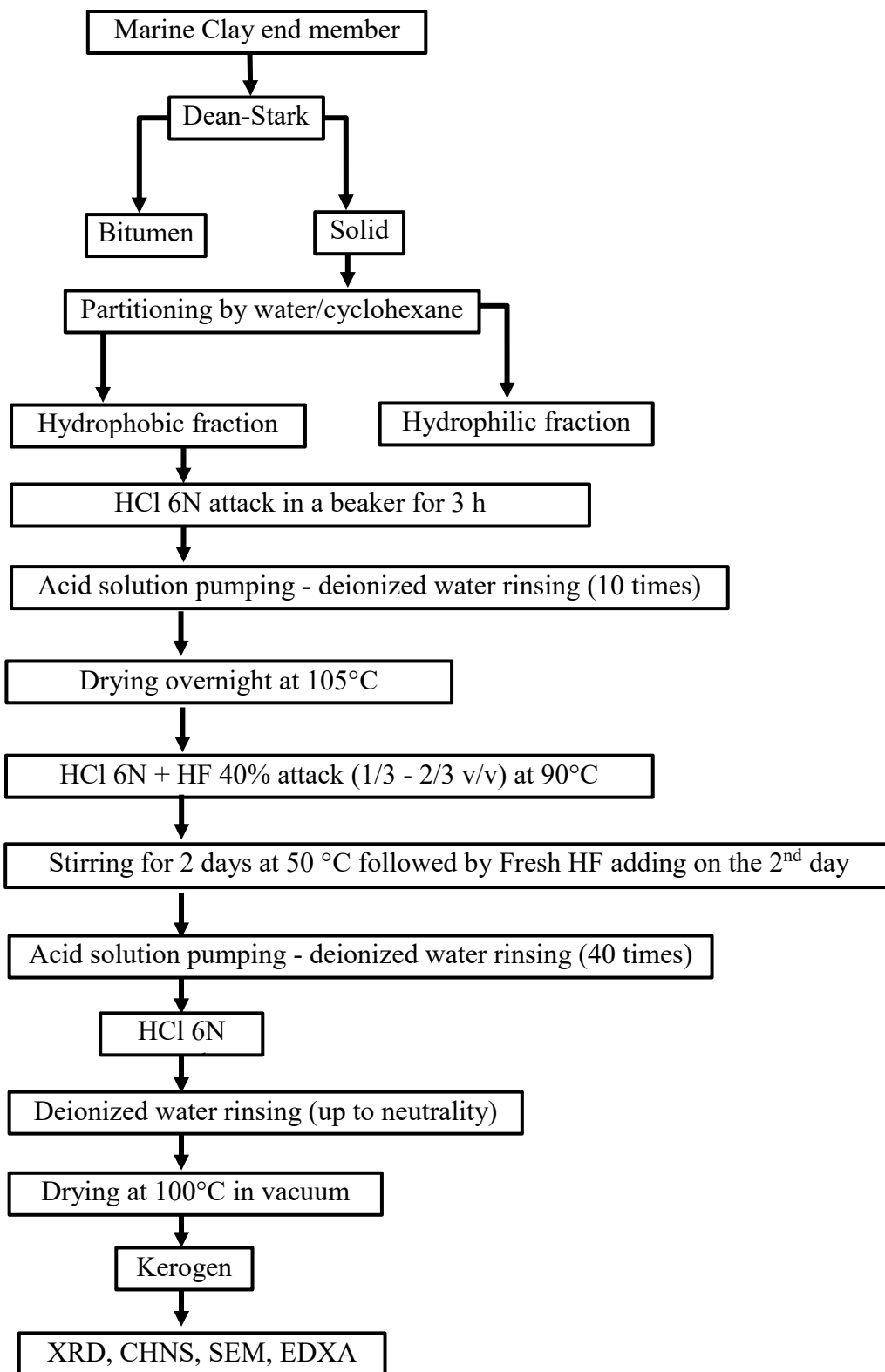


Figure 3-3: Flow diagram of kerogen extraction method and characterizing methods.

The extracted kerogen was utilized for solvent retention and sedimentation measurements by a quartz inert capillary mass spectrometer (QIC-MS) and sedimentation balance respectively, as illustrated in Figure 3-4.

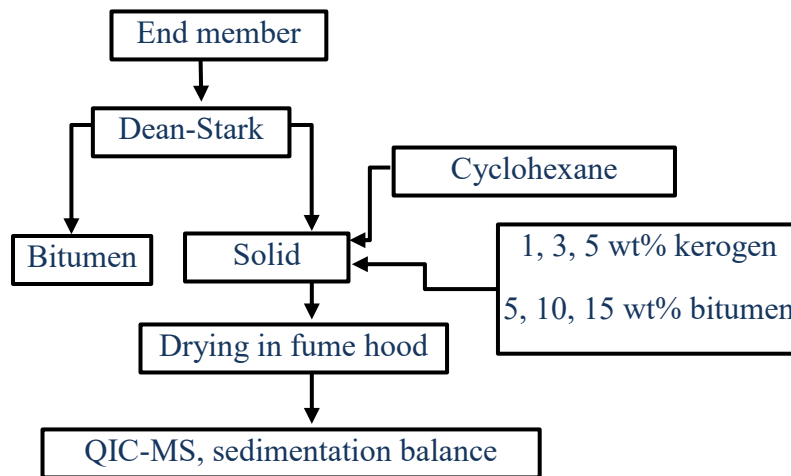


Figure 3-4: Flow diagram of sample preparation to measure solvent retention by QIC-MS and study sedimentation behavior by sedimentation balance.

3.2 Characterization methods

3.2.1 Random orientation X-ray diffraction

A Rigaku Ultima IV diffractometer was used to study the mineralogical composition of bulk samples and the various size fractions for the end members. Solids were gently ground with a mortar, sieved with a 250 μm sieve and loaded into an XRD side loading holder, which was against frosted glass. X-ray diffraction was performed from $2\theta = 4^\circ$ to $2\theta = 65.5^\circ$. The XRD profiles were then analyzed with JADE 9 software. Extracted XRD profiles from JADE 9 were used in RockJock-11 program to obtain a semi-quantitative X-ray diffraction without internal standard. The quantity of minerals are determined by the software by integrating X-ray diffraction intensities of individual minerals and compare them with the

intensities of quartz pattern as a standard. Quartz has a high amount in samples with sharp peaks that enable software to use it as a standard.

3.2.2 Organic elemental analysis

A Flash 2000 organic elemental analyzer using Eager Xperience software was used to determine the total C, H, N and S contents of the samples. All samples were dried overnight in a vacuum oven at 60°C and then ground gently to make them homogeneous. 12-15 mg of each sample were placed in an aluminum dish, then the aluminum dish was creased and sealed to hold the sample securely. Then samples were catalytically combusted in sequence at 1800°C. A chromatographic column separated the combustion products, i.e., CO₂, H₂O, N₂ and SO₂ that were then fed into a thermal conductivity detector to be quantified. To obtain accurate results, five replicates of each sample were prepared and measured; these values were averaged. By applying an acid washing process, total organic and inorganic carbon were also obtainable. The samples without acid leaching provided total carbon contents. By adding HCl to the samples, inorganic carbon (carbonates) is eliminated and only organic carbon remains in the sample. The acid treated samples provide total organic carbon contents. By subtracting organic carbon content from total carbon content, inorganic carbon content was calculated.

3.2.3 Scanning electron microscopy (SEM)

A Zeiss EVO MA 15 SEM equipped with a Bruker energy dispersive X-ray (EDX) silicon drift detector was used in this study. Before loading samples to the SEM, a thin electrically conductive carbon film was coated on their surfaces using a Leica EM SCD005

carbon coater. The coated specimen was loaded into the SEM. Elemental microanalysis was obtained at 20 kV.

3.2.4 Solvent retention analysis using QIC-MS

Residual solvents in samples, vaporized and transferred by a thermal sample collection apparatus (Short Path Thermal Collection System, Scientific Instrument Services Inc., Ringoes, NJ), were measured by a Quartz Inert Capillary Mass Spectrometer (HPR 20 QIC R & D, Hiden Analytical, Warrington, England). The thermal desorption unit of the setup is capable of operating in the range of 21-80°C; in this research samples were loaded at 50°C. Solid samples (5 g) were loaded into glass tubes and then the tubes were inserted in the thermal sample collector. High purity nitrogen gas with a flow rate of 18 ± 1 mL/min and pressure of 2×10^{-6} torr carried residual solvent in the sample to the mass spectrometer. The mass spectrometer provided a solvent gas pressure over time graph for each sample, which was converted to solvent mass in ppm by using calibration graphs. Calibration graphs were obtained by injecting known volumes of solvent into 5 g of bitumen free sample, running the process and recording the graph. Subsequently, peak integral vs. the injected volume of the solvent was plotted for several known volumes of the injected solvent. By comparing the peak integral of each unknown sample to the calibration graph, the mass of residual solvent in ppm was calculated.

3.2.5 Particle size distribution analysis

A laser particle size analyzer (Mastersizer 3000, Malvern Instruments, Westborough, MA) was utilized to determine the particle size distribution of the solid samples; i.e.,

bitumen free oil sands samples, their fractions and kerogen. The determined particle size distribution was in the form of volume fraction or number of the solids. To get comparable results for all samples, 0.5 g of solid was mixed with deionized water, followed by 15 min of homogenizing in an ultrasonic bath. Samples were mixed just before transferring to the Mastersizer and drop by drop added to obtain 5-10% obscuration. This laser beam obscuration is a measure of the added sample concentration to the instrument, with a lower limit defined to obtain better signal to noise ratio and an upper limit to prevent multiple scattering artifact. A combination of an internal ultrasound sonication and stirring was used for 1 min followed by stirring during data collection to keep particles dispersed, while a red and blue laser beam was radiated on the particles and scattered. The scattering data were used to calculate the particle size distribution in the samples.

3.2.6 Settling rate measurement

A KRÜSS K100 tensiometer is capable of being used as a sedimentation balance. The particle settling rate is a reliable substitute for graduated cylinder settling experiments. In this method a probe at a fixed location from the liquid surface collected settling particles. The measuring probe was connected to a sensitive balance that recorded weight changes. A sketch of the experimental setup is shown in Figure 3-5. The objective here was to understand the relationship between the solids settling rate and the type of hydrocarbon solvent or water that was used, and the amount of kerogen and bitumen in the samples. Solid samples, i.e., bitumen free oil sands, oil sands end members with known amounts of bitumen and kerogen, were added to water or solvent, followed by 15 minutes of sonication and stirring to prepare a suspension of evenly dispersed solids in the liquid media. For all

samples, 100 cc of the prepared suspension was poured into designated beakers of the equipment, stirred for 1 min and then the weight of settled particles was recorded over time. As the particles aggregated and settled, the solids content on the probe increased over time. The weight change of the probe is an accurate measure of the solid content as time passes.

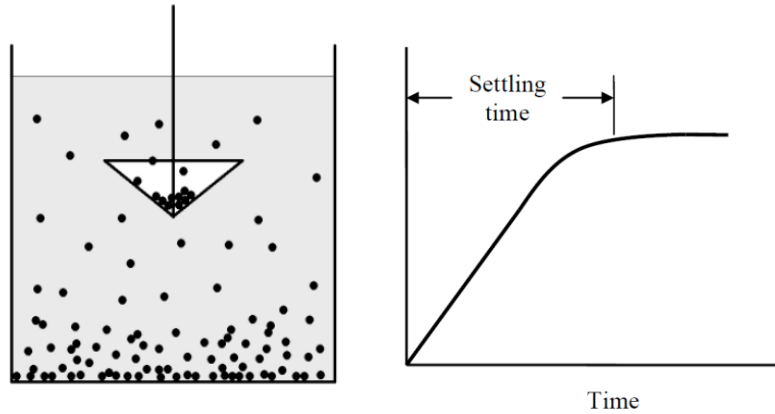


Figure 3-5: Schematic of sedimentation apparatus and resulting mass vs. time graph.

4 Results and discussion

4.1 Oil sands end members

Oil sands in this study were obtained from Syncrude's North Mine and Aurora Mine. The oil sands geological end members were disaggregated and homogenized. All end members were subjected to standard Dean-Stark extraction to extract the bitumen and at the same time, by utilizing a water trap in the apparatus, the water content was also measured. Table 4-1 shows the water content, bitumen content and solid content of different end members from Syncrude's North Mine and Aurora Mine. Significantly higher bitumen content was obtained in sand end members, whereas the water content was higher in clay end members.

To choose the best candidate for kerogen isolation, after Dean-Stark extraction, end members were analyzed for the organic carbon content. A higher amount of organic carbon content in the end member corresponded to a richer kerogen content. For this purpose, bitumen free solids from all end members after Dean-Stark extraction were analyzed by elemental analysis with and without HCl treatment.

Bitumen free end members right after Dean-Stark extraction were analyzed by elemental analysis to measure the total carbon content of the samples, including the inorganic carbon in the form of carbonates and organic carbon in the form of kerogen. Then end members were treated with HCl to leach out the inorganic carbons (carbonates) from the end members, leaving the organic carbons behind. These HCl treated samples were used to measure the total organic carbon content of the end members by elemental analysis. As summarized in Table 4-2, the highest organic carbon content was found in marine clay end members from both mines. These marine clay end members should be the best

candidates to isolate kerogen due to their higher amount of kerogen. For this study, the Aurora Mine marine clay was chosen due to its higher TOC and lower TC, which shows lower inorganic carbon that should have been leached out.

Table 4-1: Bitumen, water and solid contents of all end members from Syncrude’s North Mine and Aurora Mine.

	Sample	Bitumen (wt%)	Water (wt%)	Solids (wt%)
North Mine	ES	16.8	1.1	81.9
	EC	0.7	4.9	94.1
	MS	8.3	1.2	90.3
	MC	3.7	5.4	90.5
Aurora Mine	ES	9.6	2.9	87.1
	EC	0.15	3.4	96.1
	MS	8.9	3.7	87.3
	MC	5.6	5	89.3

Table 4-2: Total carbon content (TC) and Total organic carbon content (TOC) for all end members measured by CHNS before and after HCl treatment, respectively.

	Sample	TC (wt%)	TOC (wt%)
North Mine	ES	0.51	0.46
	EC	1.59	1.25
	MS	2.25	1.87
	MC	4.12	3.63
Aurora Mine	ES	0.93	0.81
	EC	1.58	1.43
	MS	1.24	1.06
	MC	3.73	3.65

4.2 Kerogen extraction and characterization

4.2.1 Homogenizing and Dean-Stark extraction

In order to extract kerogen from Aurora Mine marine clay, oil sands samples were prepared by grinding to pass a 60 mesh sieve and homogenizing. The homogenized marine clay was subjected to Dean-Stark extraction for 12 h to remove all the bitumen in the samples. Several Dean-Stark extractions showed a consistency in bitumen content and water content of the prepared samples, as illustrated in Figure 4-1 and Figure 4-2, verifying that the homogenizing during sample preparation was effective. The average bitumen content and water content that are listed in Table 4-3 are also consistent with the previous screening test.

Table 4-3: Bitumen, water and solid contents in oil sands marine clay end member from Syncrude's Aurora Mine.

Aurora Mine marine clay	Bitumen (wt%)	Water (wt%)	Solids (wt%)
Average	5.57	5.03	89.39
STDEV	0.38	0.26	0.18

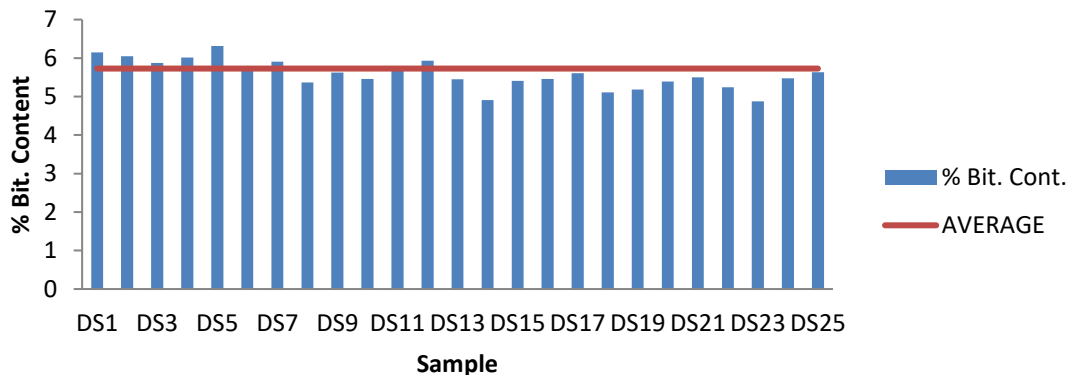


Figure 4-1: Bitumen content (wt%) in oil sands marine clay end member from Syncrude’s Aurora Mine.

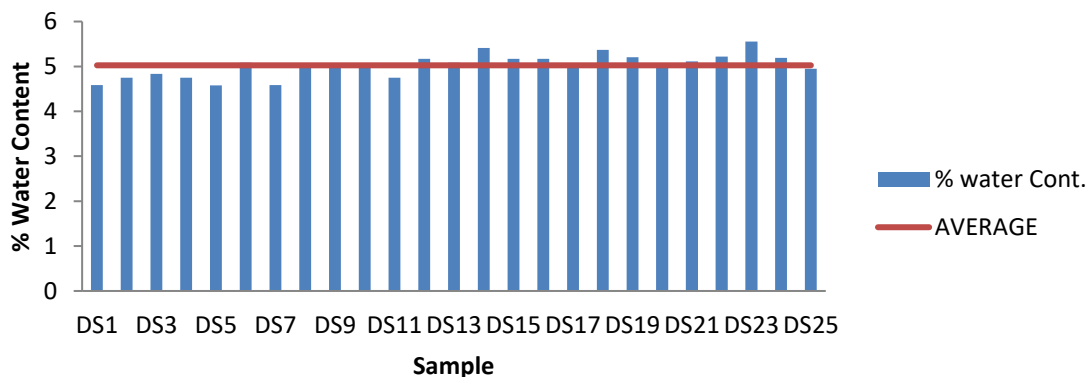


Figure 4-2: Water content (wt%) in oil sands marine clay end member from Syncrude’s Aurora Mine.

4.2.2 Bitumen free oil sands particle fractioning

In order to reduce the amount of acid leaching in the process of kerogen extraction, which includes HCl treatment followed by HF/HCl treatment, a novel particle fractioning was developed. Attempts were made to separate particles with higher amounts of kerogen from other clay particles based on their difference in hydrophobicity. For this purpose the bitumen-free marine clay after Dean-Stark (MC-DS) samples were subjected to water sedimentation with air bubble frothing and also water/cyclohexane fractioning. Figure 4-3 shows the fractioning samples in water and water/cyclohexane. Water/air bubble

fractioning was not possible because no distinct separation had occurred and a collectable froth was not created. On the contrary, the water/cyclohexane mixture provided two immiscible fractions that could easily be separated by syphoning from the top. The hypothesis is that kerogen containing particles are more hydrophobic and based on their hydrophobicity would accumulate in the cyclohexane fraction and float to the upper fraction of the container while other particles which are more hydrophilic will settle down into water. These two fractions were separated for further analysis.

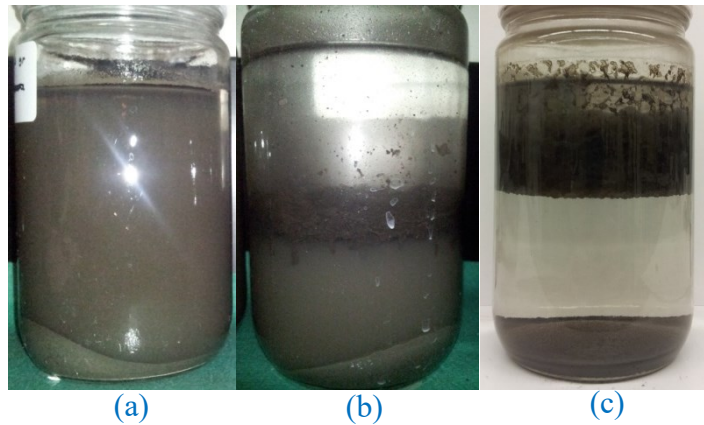


Figure 4-3: Partitioning of MC-DS based on hydrophobicity. (a) In water, (b) in water/cyclohexane after 1 h, (c) in water/cyclohexane after 24 h.

A laser particle size analyzer, Mastersizer 3000, was used to measure the particle size distribution of all fractions. After adding the sample to the Mastersizer, stirring was done at 2500 RPM with ultrasound sonication for 1 min and then sonication was stopped and the stirring speed was lowered to 1000 RPM to start the particle size distribution measurements. Bitumen free marine clay samples show a wide range of particle sizes, so that larger particles settle quickly. Figure 4-4 shows the particle size distribution for MC-DS after different periods of stirring at 1000 RPM. The first measurement shows three peaks at around 20, 200 and 2000 μm , while after 5 min of stirring at 1000 RPM larger

particles settled and the peaks at ~ 200 and $\sim 2000 \mu\text{m}$ were eliminated. Also Figure 4-5 shows a rapid and significant drop in the particle size distribution of MC-DS. $D_x(90)$ percentile shows that 90% of all particles are smaller than $450 \mu\text{m}$ at start and after 5 min it drops to $50 \mu\text{m}$ that means larger particles are settled.

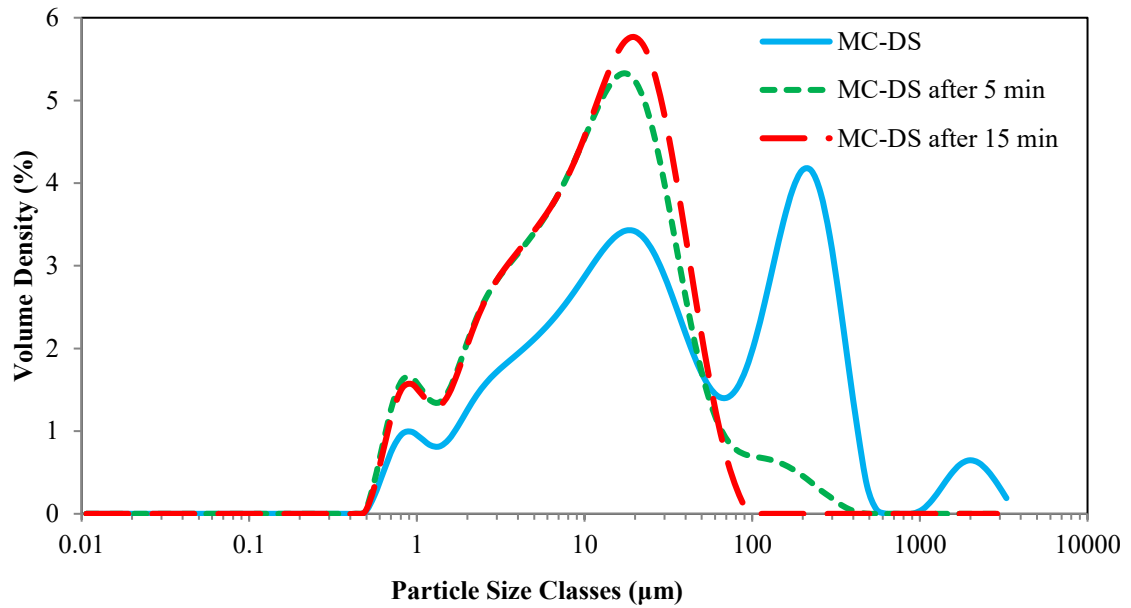


Figure 4-4: Particle size distribution for marine clay after Dean-Stark (MC-DS) for different time periods.

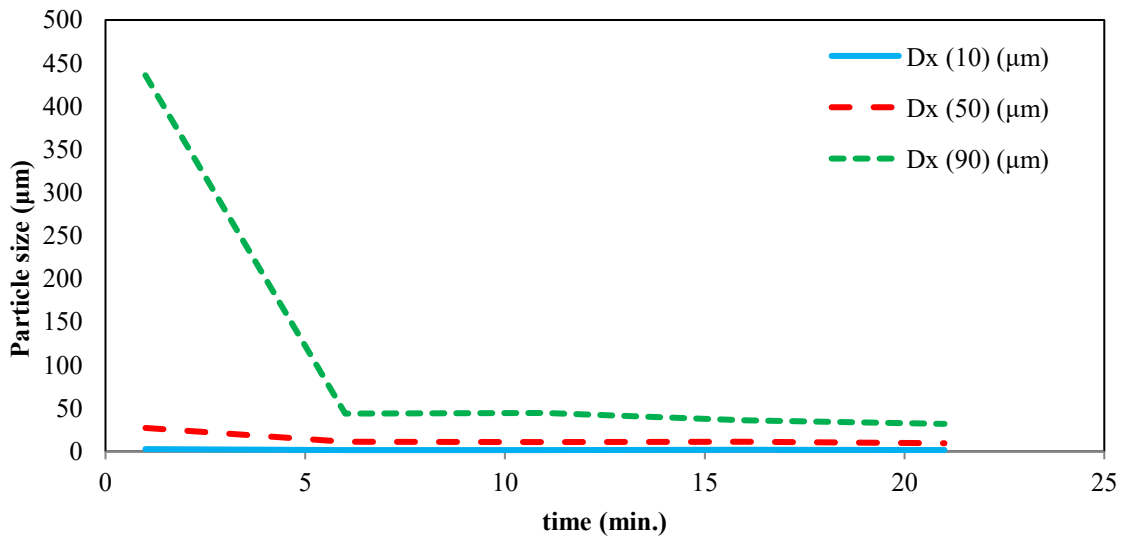


Figure 4-5: MC-DS particle size percentiles for different time periods.

To analyze the size distribution of the hydrophobic and hydrophilic fractions of MC-DS, the fractions were agitated and sonicated for 10 min. Two samples were chosen for the Mastersizer for each fraction, one at the middle of the container, which has finer particles, and the other from the bottom of the container that includes coarser particles. Figure 4-6 shows the particle size distribution for marine clay hydrophilic (MC-L) and marine clay hydrophobic (MC-B) fractions. The size distribution of MC-L is a representative of the MC itself with a wide range of fine and coarse particles. The size distribution of MC-B was limited to fine particles. However, there was no significant difference in size distribution for the MC-L fine fraction and MC-B fine and coarse fractions. Table 4-4 summarizes the average particle size distributions for the MC-B and MC-L fractions. The results show a wide range of particle size (from 39 to 440 μm) for the hydrophilic fraction (MC-L), but a narrower size distribution for the hydrophobic fraction (MC-B; 35 to 46 μm).

Table 4-4: Average size distributions for MC-DS partitions in water/cyclohexane.

<i>sample</i>	<i>Dx 10 (μm)</i>	<i>Dx 50 (μm)</i>	<i>Dx 90 (μm)</i>
MC-L fine	1.82	11.95	39.40
MC-L coarse	17.10	246.17	436.50
MC-B fine	1.81	10.25	35.70
MC-B coarse	1.95	11.96	45.22

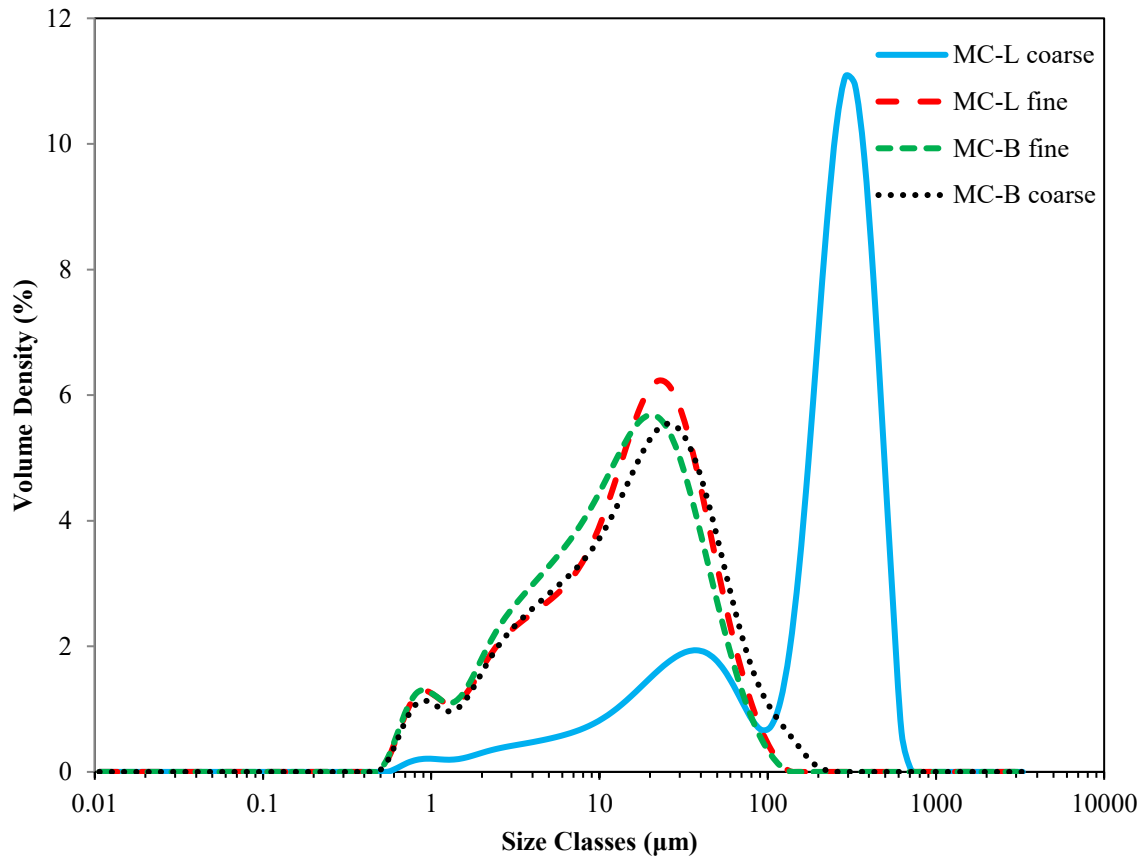


Figure 4-6: Particle size distribution for hydrophilic (MC-L) and hydrophobic (MC-B) fractions of MC-DS.

XRD patterns from MC-DS and MC-B are shown in Figure 4-7 and indicate that the inorganic composition of the hydrophobic fraction is almost the same as the marine clay itself, except that the hydrophobic fraction has a lower amount of quartz.

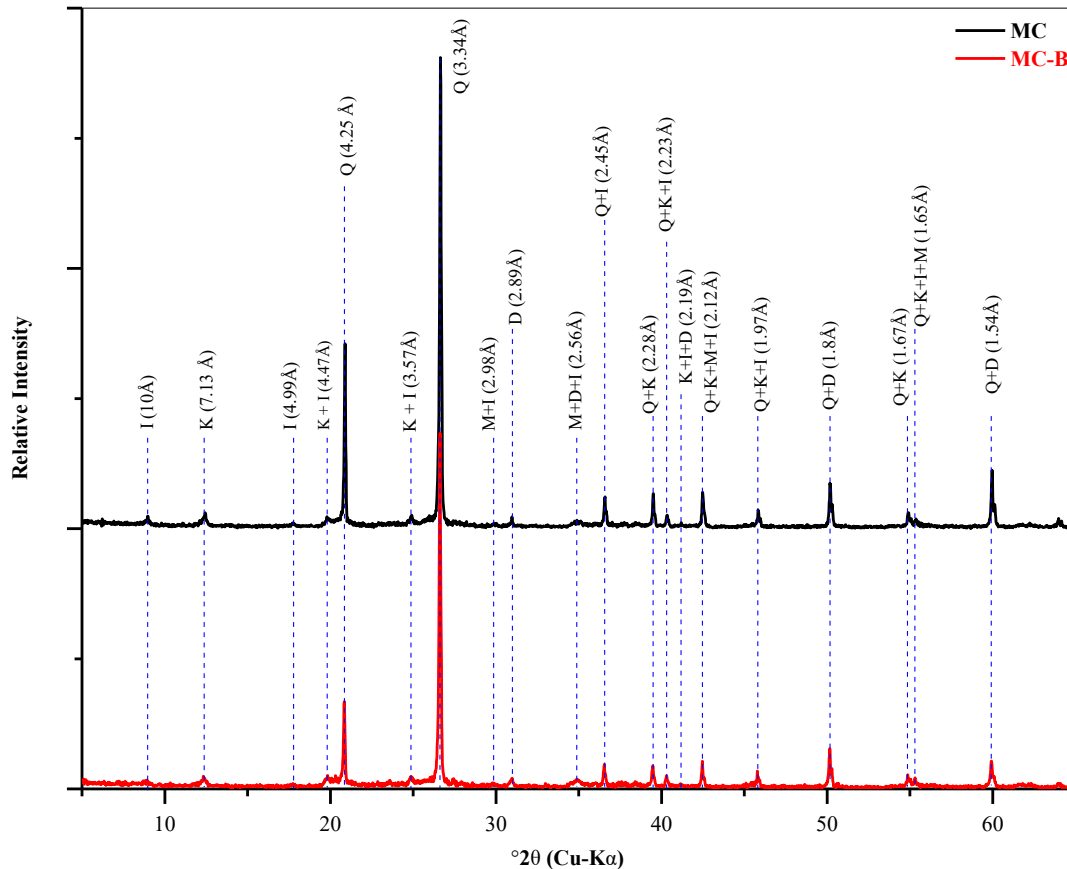


Figure 4-7: XRD patterns for random preparations of bulk samples of MC-DS and MC-B. I, illite; K, kaolinite; Q, quartz; D, dolomite; M, magnetite.

To see the distribution of organic carbon in the hydrophilic and hydrophobic fractions, total carbon content of the samples from both fractions was measured by CHNS elemental analysis. Then samples from both fractions were treated with concentrated HCl for 3 h. The samples were then rinsed four times to remove any dissolved carbonate and analyzed by CHNS elemental analysis to measure the total organic carbon content. Figure 4-8 shows the total carbon content (TC) of the samples, which revealed a higher carbon content in the hydrophobic fraction. Figure 4-9 shows the carbon content of the samples after HCl treatment and elimination of carbonates. Interestingly, there was no organic carbon in the

hydrophilic fraction, confirming that all the kerogen is accumulated in the hydrophobic fraction and hydrophilic particles are clays containing carbonates.

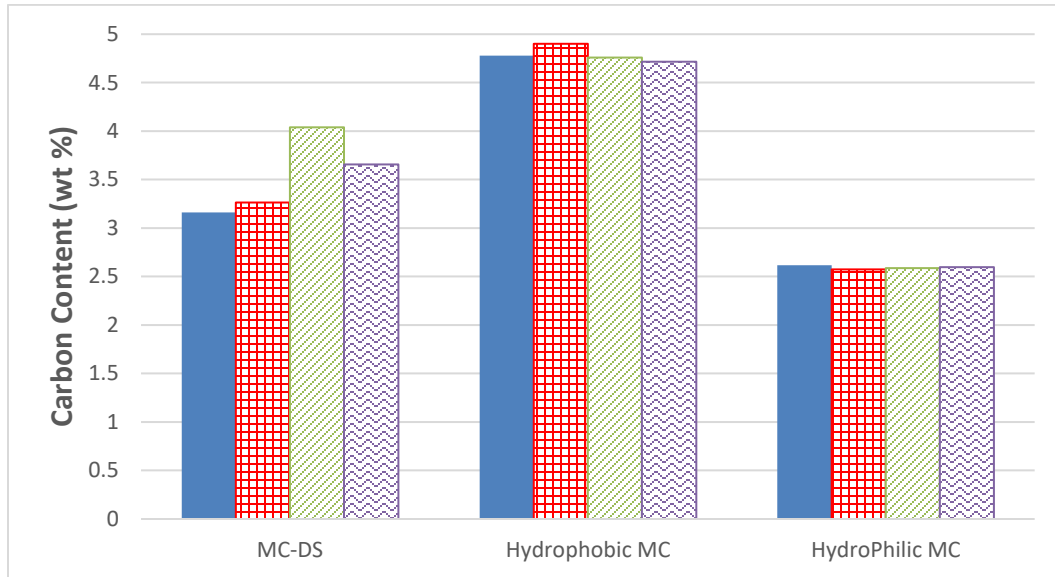


Figure 4-8: Total carbon content of marine clay samples measured by CHNS before HCl treatment.

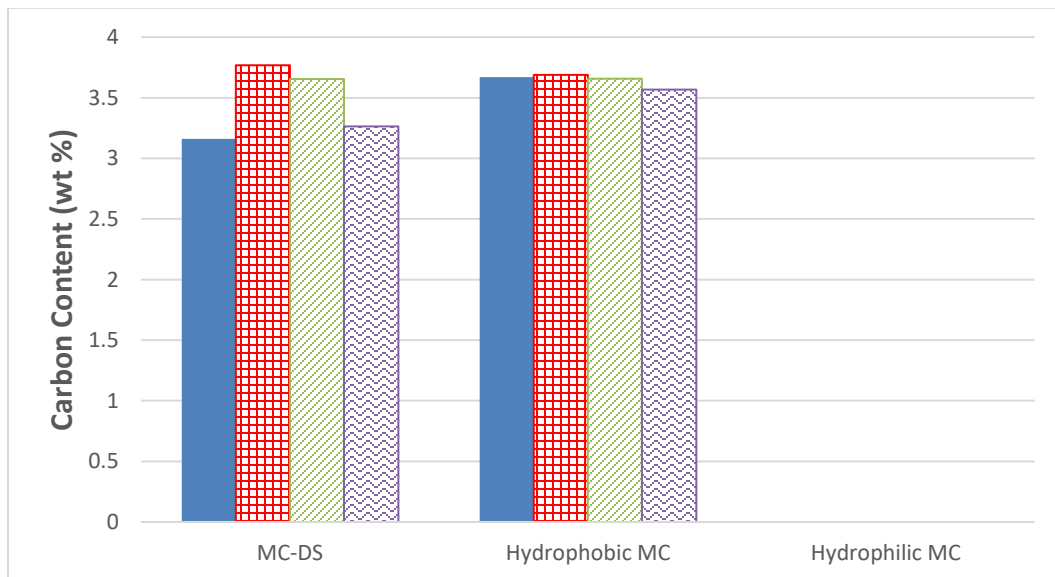


Figure 4-9: Total organic carbon content of marine clay samples measured by CHNS after HCl treatment.

The XRD pattern of the MC-B sample after HCl treatment (MC-HCl) (Figure 4-10) also shows the elimination of dolomite, which is the inorganic carbonate in marine clay.

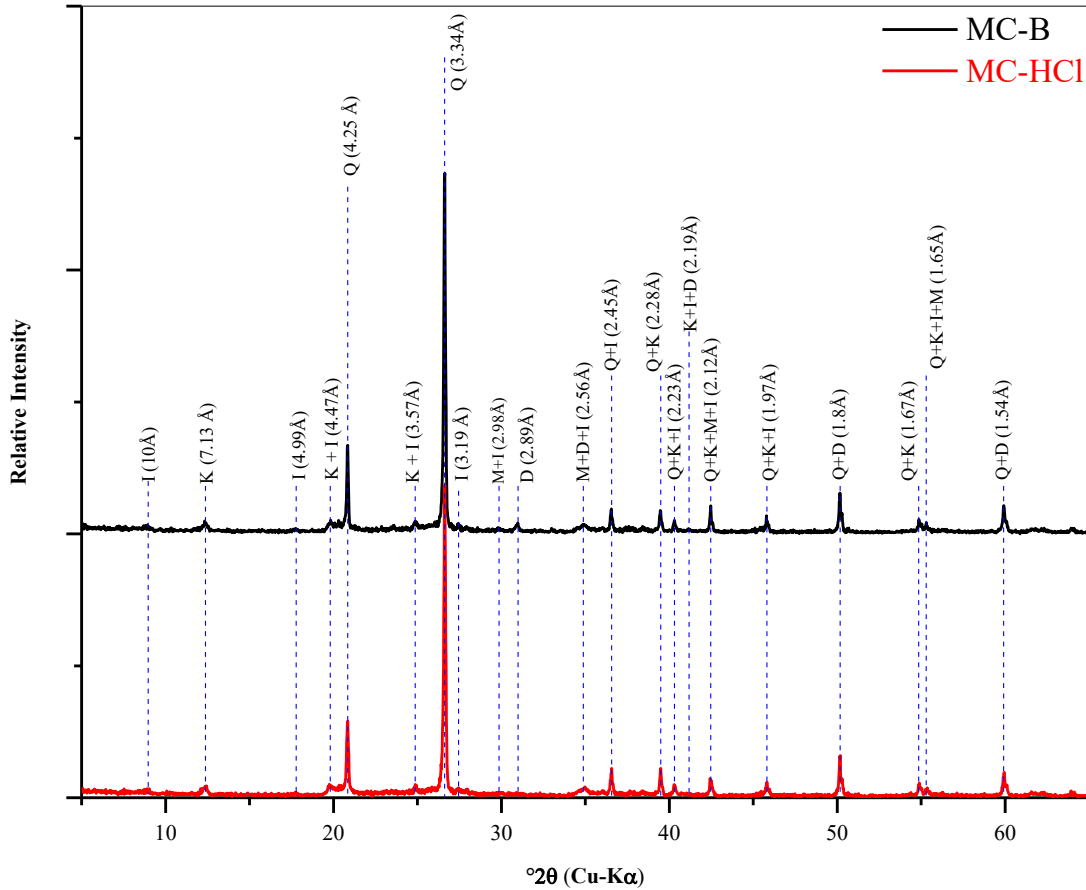


Figure 4-10: XRD patterns for random preparations of bulk samples of MC-B and MC-HCl. I, illite; K, kaolinite; Q, quartz; D, dolomite; M, magnetite.

4.2.3 Acid leaching of hydrophobic marine clay fraction

To examine the effectiveness of different acid leaching processes, three sets of marine clay after Dean-Stark extraction (MC-DS) were exposed to HCl, HF and HCl-HF. The samples were prepared by mixing 20 g of MC-DS with 100 mL deionized water, followed by adding 50 mL of the designated acid to the mixture. After two days of exposure to acid,

samples were washed with deionized water to neutral pH and characterized by SEM equipped with an EDX detector. Si is an indicator of quartz and the Si content of the samples was used as a marker to evaluate the effectiveness of the acid leaching process. EDX analysis results are presented in Table 4-5, which show the lowest content of Si in samples exposed to HCl and then leached by HF as proposed in the literature, while exposing to HF alone is not favorable. However, the Si content is very high in all three sets of samples. To make acid leaching more effective for Si elimination, after one cycle of acid leaching with HCl, particles were dried. Then the second cycle of acid leaching with HF, which is used to eliminate quartz, was started by pouring HF on dry samples at an elevated temperature of 90°C and kept at 50-60°C for 2 days. EDX analysis of the residue particles after this hot acid leaching process showed a significant drop in Si content. In addition, a slight drop of Fe was observed, but the process had no effect on the Al content of the samples. Figure 4-11 shows EDX mapping of samples and confirms the co-presence of Fe and S as an indication of pyrite.

Table 4-5: EDX analysis results (wt%) after wet and dry hot leaching.

Sample	C	O	Mg	Al	Si	S	K	Ca	Fe
MC-DS after HCl-HF leaching	22.9	51.5	0.2	4.6	17.6	0.4	1.3	0.1	0.8
MC-DS after HF leaching	15.8	45.2	0.9	9.7	18.6	0.3	3.7	2.3	2.1
MC-DS after HCl leaching	14.5	48.7	0.3	7.7	23.8	0.4	2.2	-----	1.6
MC-B after HCl hot HF leaching	25.8	9.4	2.5	9.2	0.1	1	1.7	0.2	0.8

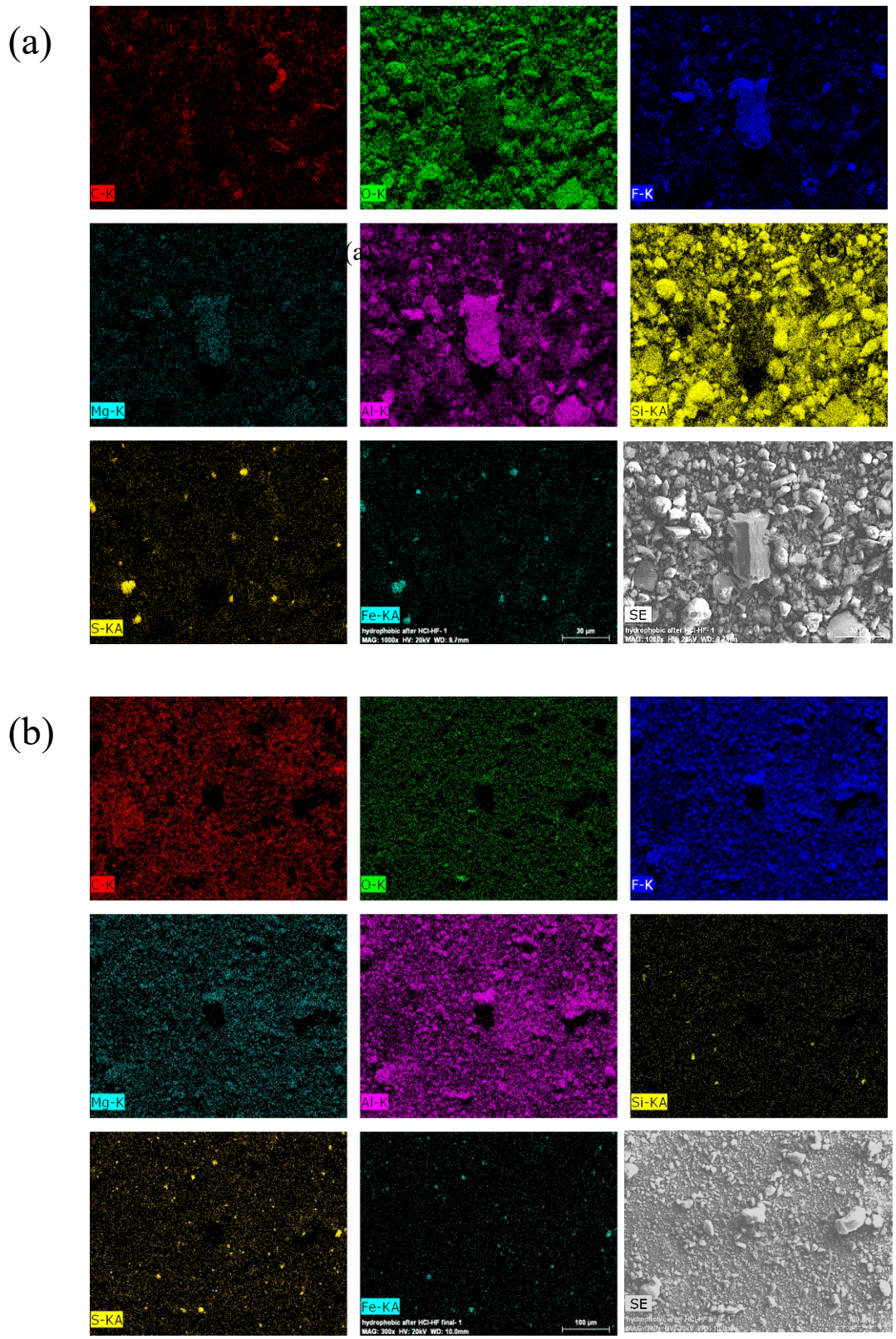


Figure 4-11: EDX mapping for MC samples after acid treatment by HCl-HF. (a) wet condition and (b) dry condition.

Based on these results to extract kerogen from marine clay, the hydrophobic fraction (MC-B) was separated by the water/cyclohexane fractioning process developed in this study. The kerogen rich fraction was treated with concentrated HCl (6 N) for 3 h with stirring, then the particles were allowed to settle for another 3 h. The solution on top of the particles was syphoned off and then the samples were rinsed 10 times with deionized water to remove any dissolved Ca ions. The residues from HCl treatment were dried overnight in an oven at 105°C. The dried particles were subsequently treated with a mixture of 45% HF and 6 N HCl with a volume ratio of 2/3-1/3, respectively, at a temperature of 90°C. The particles in the acid mixture were stirred for two days at 50 to 60°C. Fresh HF was added to the slurry on the second day. The leached residues were rinsed with deionized water to almost neutral pH (pH = 7), followed by the addition of a small amount of HCl to dissolve any possibly newly formed fluorosilicates. The remaining solids, mainly kerogen and some heavy sediments were rinsed with deionized water to neutral pH.

4.2.4 Extracted kerogen fractions analysis

The residues from the acid leaching process were separated into three fractions. After the final rinse, the container was filled with deionized water and agitated vigorously and then allowed to settle for 1 h. At this time, a vague mud line was formed near the bottom of the container. With syphoning, the top two thirds of the container were first collected and named as K-top. Then the remaining one third of the container was collected as K-low and the sediments decanted and named as heavy sediment. All fractions were dried and stored in vacuum separately for further characterization. CHNS results of these fractions are summarized in Table 4-6. The results show that kerogen fractions have higher TN/TOC ratios than the bitumen extracted from the oil sands end members from the Aurora Mine. It

has been reported that the TN/TOC ratio for bitumen is between 0.0017 and 0.01 while this ratio for asphaltene is in range of 0.012 to 0.016 ⁷². By an increase in the molecular weight of organic matter, the TN/TOC is increased and this ratio for kerogen is reported to be more than 0.019 in Aurora Mine end members ⁶⁸.

Table 4-6: CHNS elemental analysis of Aurora Mine marine clay bitumen and its different fractions of extracted kerogen.

Sample	N (wt%)	C (wt%)	H (wt%)	S (wt%)	TN/TOC
K-top	1.319	52.696	4.223	6.227	0.025
K-low	0.442	21.040	2.508	3.030	0.021
heavy sediment	0.007	0.666	0.150	0.774	0.011
Bitumen-MC	0.842	85.181	10.217	4.293	0.011

XRD patterns of the fractions are summarized in Figure 4-12 and show pyrite and chromatite as inorganic components of K-top. However, newly formed fluorides, ralstonite and rosenbergite, are present in the K-low. The fluorides that are formed during the HF treatment of the marine clay have specific densities higher than 2.4 g/cm³, which is greater than kerogen with a specific density less than 1.5 g/cm³. This difference in specific densities makes the settling of the newly formed fluorides faster than kerogen and concentrates them in K-low and heavy sediments. Newly formed fluorides also have greater particle sizes relative to the hydrophobic fraction of marine clay that was subjected to the acid treatment to extract the kerogen. Figure 4-13 shows the large newly formed fluorides in a background of smaller particles and a significantly larger amount of fluorine and aluminum content. The point EDX analysis of these large particles shows that an F:Al ratio of 1:3 in the particles, which

is attributed to the presence of ralstonite and rosenbergite in kerogen fractions revealed by XRD patterns. Also semi-quantitative XRDs are performed by RockJock 11 software on different MC and kerogen fractions. Table 4-7 summarizes semi-quantitative XRD results, which shows different amount of newly formed fluorides in kerogen fractions. Mineral composition of marine clay calculated by RockJock 11 for our samples are in agreement with previous studies on oil sands end members ^{28,36,68,72}. Quartz is the main mineral of marine clay end member as reported in previous studies. During water/cyclohexane fractioning, quartz particles are settled in the hydrophilic fraction and increase the quartz content from 59.3 wt% in MC to 66.2 wt% in MC-L; in contrary quartz concentration in hydrophobic fraction is decreased to 54.9 wt%. This decrease in quartz concentration in hydrophobic fraction reduced the acid leaching process with HF, which was the main goal of water/cyclohexane fractioning process. Carbonates including dolomite, calcite, ankerite and titanite are accumulated in the hydrophobic fraction, probably due to their particle size, particle shape or surface properties like hydrophobicity. It is in consistency with previous studies that observed carbonate minerals e.g. dolomite and calcite in the oil sands froth ^{12,72}. All of carbonates and clays are eliminated after acid leaching process that shows the effectiveness of acid leaching on carbonates and clays. It is interesting that the concentration of clay particles including kaolinite, illite and smectite are not varied significantly in hydrophobic or hydrophilic fractions, though their particle sizes are finer and expected to be accumulated in the top fraction. Kerogen-top is the most pure fraction of kerogen, although quartz is still the main inorganic that is preserved even after 2 days of HF leaching. Acid leaching residuals are concentrated in heavy sediments. It is worth to remind that semi-quantitative XRD is performed without internal standard and calculations in software are performed based on quartz peaks as a standard. This process might highlight quartz in samples especially when quartz

concentration is lower. However, it is not as accurate as quantitative XRD with internal standard, but semi-quantitative XRD is useful to compare samples. Gypsum is the next most abundant mineral in kerogen fractions. The presence of gypsum in kerogen fractions is in agreement with previous study on non-aqueous bitumen extraction from the Athabasca oil sands ⁷². The presence of pyrite is expected as an associated mineral with kerogen and in agreement with studies showed significant accumulation of pyrite and siderite in the primary froth after aqueous extraction of Athabasca oil sands ^{3,68,72}.

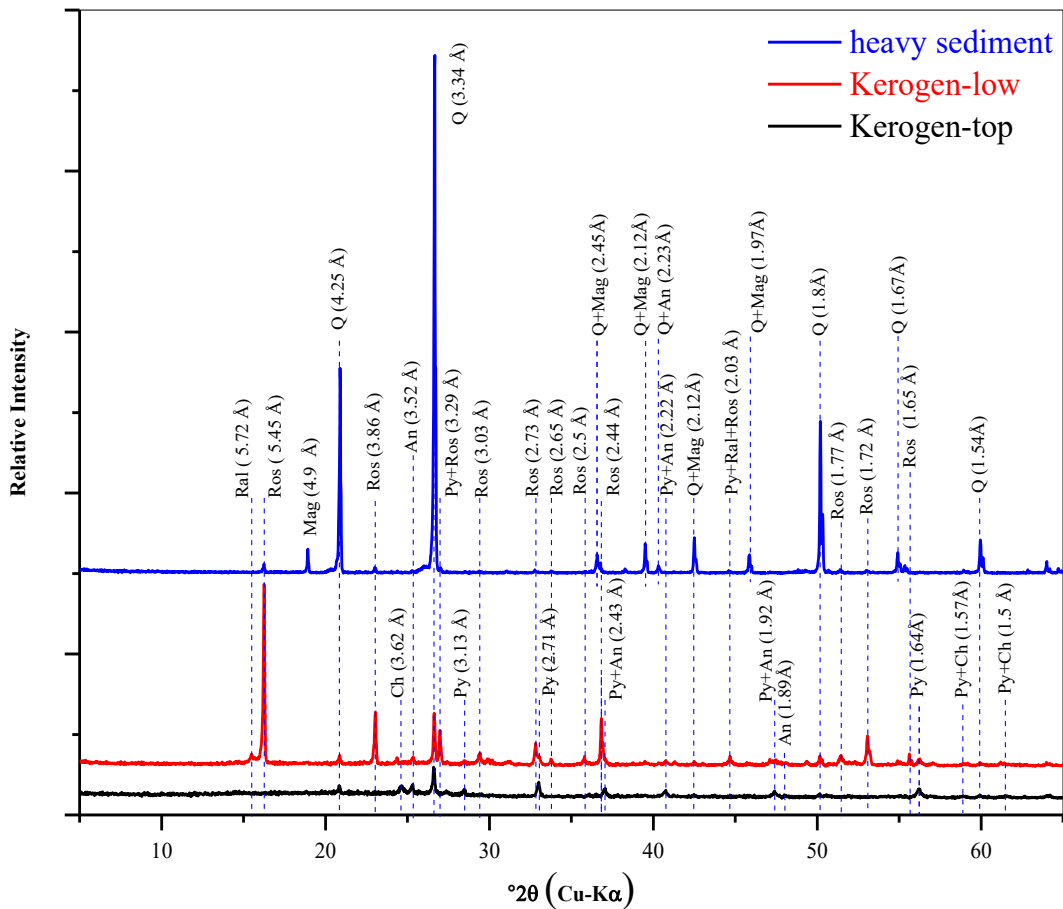


Figure 4-12: XRD patterns for random preparations of bulk samples of different fractions of kerogen extracted from Aurora Mine marine clay. Ral, ralstonite; Ros, rosenbergite; Mag, magnetite; Ch, Chromatite; An, annite; Py, pyrite; Q, quartz.

Table 4-7: Mineral composition (wt%) of different fractions of Aurora Mine marine clay and kerogen determined by RockJock 11 software.

Mineral		MC	MC-B	MC-L	K-Top	K-Low	Heavy Sed.
NON-CLAYS	Quartz	59.3	54.9	66.2	19.6	47.6	72.9
	Dolomite	6.8	14.9	6.2	0.0	0.0	0.0
	Other Carbonates	11.2	13.4	10.4	0.0	0.0	0.0
	Fe bearings	1.2	0.7	0.1	0.0	0.0	3.1
	Pyrite	0	0	0	1.7	1.8	2.3
	Gypsum	0	0	0	10.2	11.1	16.5
	Newly formed Fluorides	0	0	0	1.2	2.2	1.3
	Ti bearings	0	0	0	0.6	0.5	3.3
	Carbon rich	0	0	0	12.6	15.3	0.0
Total non-clays	78.5	83.9	82.9	46.0	78.5	99.3	
CLAYS	Kaolinite	3.3	2.5	6.2	0	0	0
	Smectite	3.1	1.0	6.5	0	0	0
	Illite	15.1	12.5	4.4	0	0.0	0.0
Total clays	21.5	16.0	17.1	0.0	0.0	0.0	

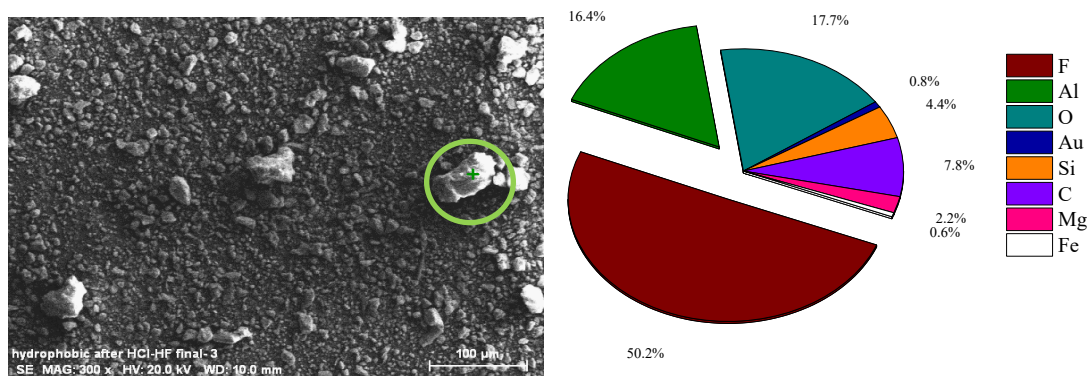


Figure 4-13: Secondary electron image of SEM and EDX analysis of the newly formed fluorides after HCl-HF treatment of marine clay.

4.3 Solvent retention by kerogen

4.3.1 Sample preparation

The as-received petrologic end members from the Aurora Mine of Syncrude Canada Ltd. (Fort McMurray, Alberta) were manually disaggregated and passed through a sieve with an aperture size of 6.35 mm, then homogenized and stored frozen in sealed containers. For this part of the experiment, the prepared Aurora Mine marine clay samples were defrosted at room temperature (20-25°C) in sealed containers overnight. Dean-Stark extraction was performed and bitumen-free solids were collected as MC-DS, dried at 60°C for 24 h and ground gently to disaggregate the possible lumps.

4.3.2 Drying time measurement

A 10 g sample of MC-DS was mixed with 9 mL of cyclohexane (ratio of 60:40 wt%, respectively) in a petri dish and placed on a balance, which was connected to a computer. In a fume hood at room temperature (21-25°C), every 30 s the weight was recorded to obtain the weight loss of the sample (Figure 4-14). It is clear that solvent evaporation was fast at the start, following an almost linear trend and then slowed to reach a constant value. To obtain the time for the convergence to a constant weight, the derivative of the total weight loss was calculated numerically and its intercept with zero was determined, which shows that the total weight loss is constant. For the results with MC-DS and cyclohexane, the time of zero total weight loss happened after 30 min. Therefore, drying time of sample preparation was set to 60 min as a conservative time frame.

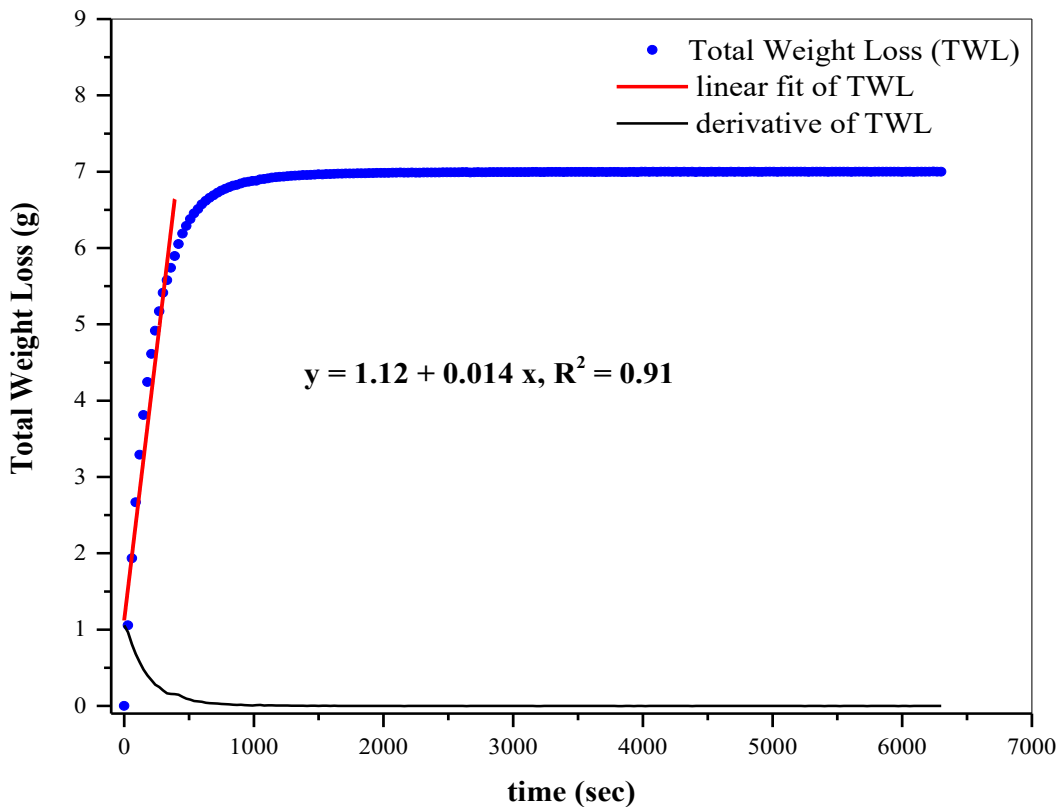


Figure 4-14: Total weight loss of MC-DS sample saturated with MC-DS:cyclohexane ratio of 60:40.

4.3.3 Sample preparation for solvent retention experiments

For each measurement, 5 g of MC-DS was weighed, mixed with 4.5 mL cyclohexane and placed in a petri dish in a fume hood for 1 h to let the sample dry. To see the effect of different amounts of kerogen in solvent retention, further samples were prepared by adding 1, 3 and 5 wt% to the MC-DS, followed by mixing and then the addition of cyclohexane. Finally, dried samples were packed into glass tubes to load into a thermal sample collection apparatus (Short Path Thermal Collection System, Scientific Instrument Services Inc., Ringoes, NJ) with glass wool at the two ends. Desorbed gas from the sample (including water, oxygen, carbon dioxide, toluene and cyclohexane) was carried out by a flow rate of 18 ± 1 mL/min of high purity nitrogen gas. This gas was delivered to a quartz inert capillary mass

spectrometer (HPR 20 QIC R & D, Hiden Analytical, Warrington, England) working at a pressure of 2×10^{-6} torr for the duration of the analysis. Figure 4-15 shows the results of QIC-MS for MC-DS mixed with cyclohexane. Zero intensity for oxygen and carbon dioxide shows that the glass tube was completely sealed in the QIC-MS and no leakage happened. The presence of water and toluene is due to the connate water of the oil sands and remaining solvent from Dean-Stark extraction, respectively.

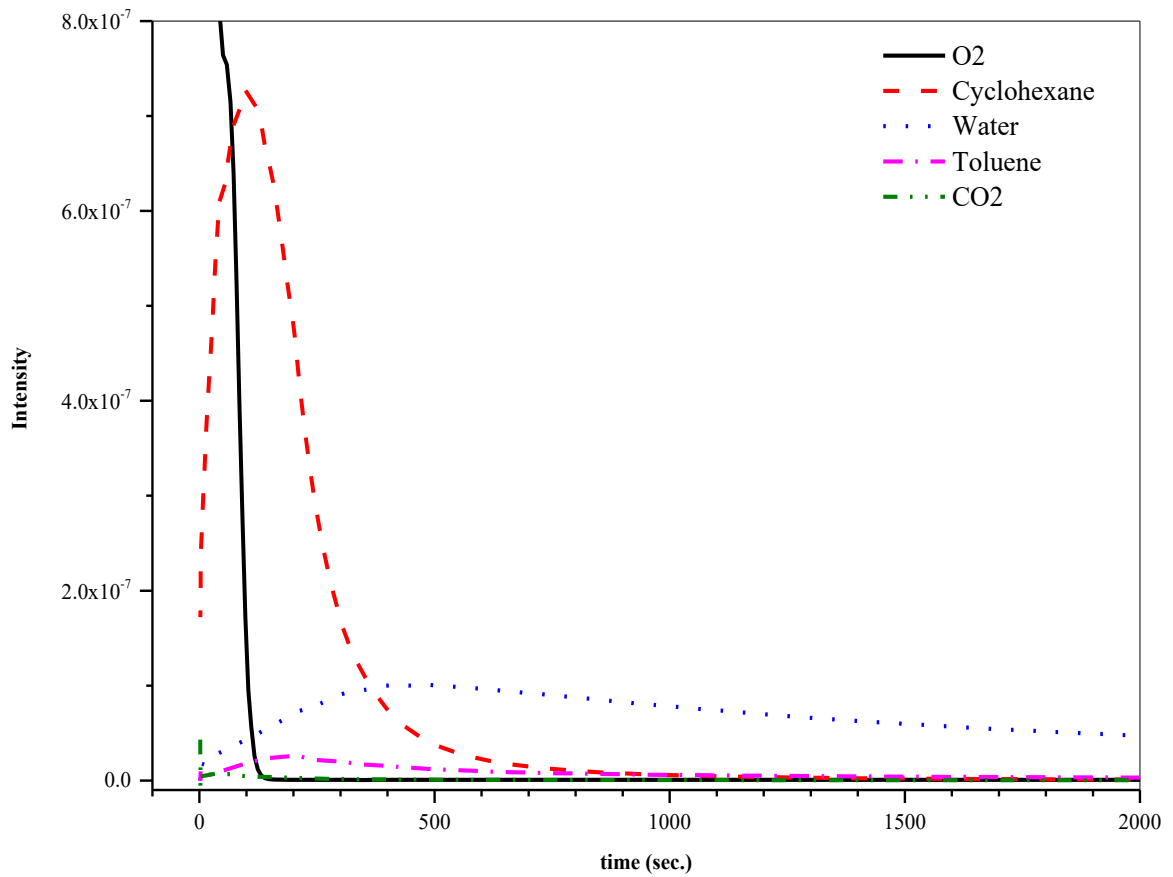


Figure 4-15: QIC-MS results for desorbed gases from MC-DS mixed with cyclohexane.

4.3.4 Calibration equation of QIC-MS response with cyclohexane

In order to convert the intensity response of QIC-MS to the actual content of the desorbed solvent, a calibration diagram and derived equation of the calibration line are necessary. This diagram was generated by injecting known volumes of cyclohexane to 5 g of MC-DS and collecting the QIC-MS responses. Then the mean peak integral of the QIC-MS responses were plotted against the injection volume of cyclohexane to obtain the calibration curve. The injected amount of cyclohexane ranged between 100 and 1300 μL . Figure 4-16 shows the calibration plot generated from the data points resulting from injecting known volumes of cyclohexane in the QIC-MS setup and their fitted line. The formula for the fitted line was used to determine the actual volume of desorbed cyclohexane, based on the QIC-MS responses, for samples with different kerogen contents. The derived equation is consistent with the previous study by Siddhant ⁷³.

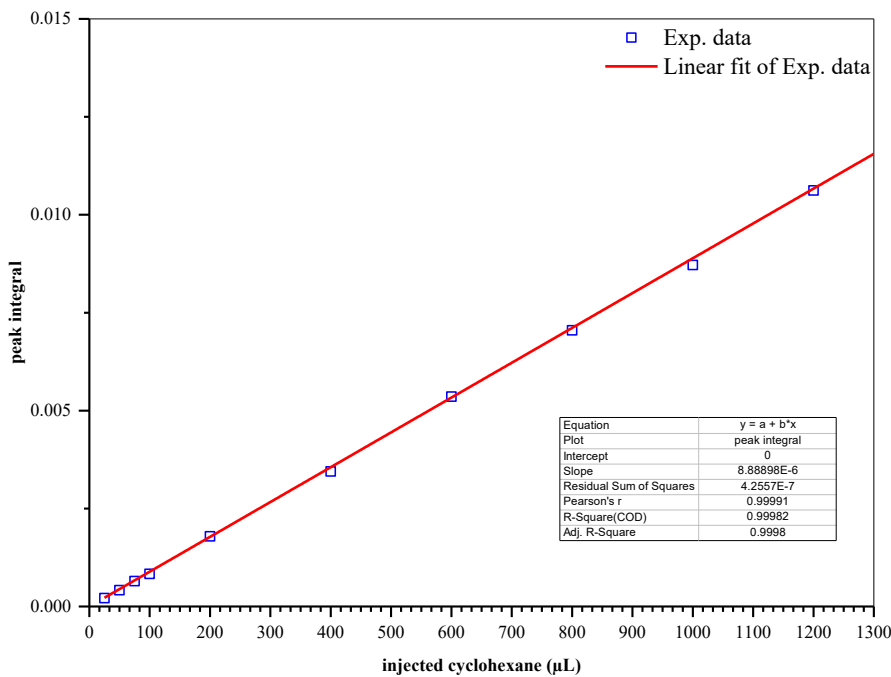


Figure 4-16: Calibration plot of QIC-MS response for known volumes of cyclohexane.

4.3.5 Cyclohexane desorption results

For each kerogen content, 3 samples were prepared and the residual cyclohexane was measured by the QIC-MS setup. Figure 4-17 shows the average of QIC-MS responses for all samples. There is a significant correlation between kerogen content and solvent retention; increasing the kerogen content in the oil sands samples results in higher solvent retention. In addition, there is a slight difference in the elapsed time before cyclohexane is released completely. Higher kerogen content also makes the process of solvent evaporation more time consuming as shown in Figure 4-18. It shows that by increasing the kerogen content and subsequently by having more residual solvent in samples, longer time is elapsed to evaporate all of the retained solvent. However in slightly shorter times solvent release gets to its maximum rate which the QIC-MS response peak happens.

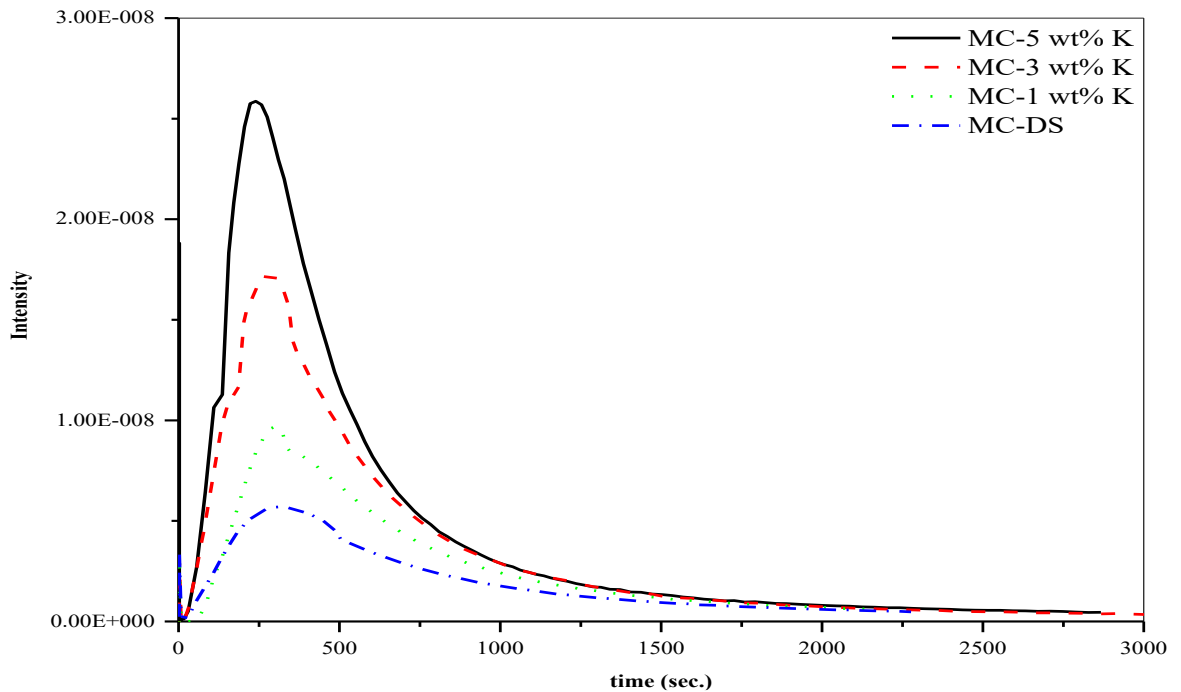


Figure 4-17: Average responses of QIC-MS for samples with different kerogen contents.

Based on the QIC-MS results and the calibration plot with the fitted line, the residual solvent was calculated and the results are presented in Table 4-8. More residual cyclohexane is attributed to higher kerogen contents. It is in consistency with previous studies that attributed solvent retention in oil sands to fine particles^{74,75} and bitumen content⁷³. It's been revealed that by increasing fine particles the residual solvent would be higher, also by increasing the bitumen content higher residual solvent has been reported. In our study kerogen as a high molecular weight organic structure acts similar to bitumen and holds more solvent in the samples with higher kerogen content. Total residual solvent in different samples are ranged from 80 to 226 ppm which is comparable to previous studies^{20,73,74}. This residual solvent is extremely lower than the current limit of solvent loss per bitumen production, for existing water-based extraction method. The Alberta Energy Resources Conservation Board sets the limit of solvent loss less than four volumes per thousand volumes of bitumen production.

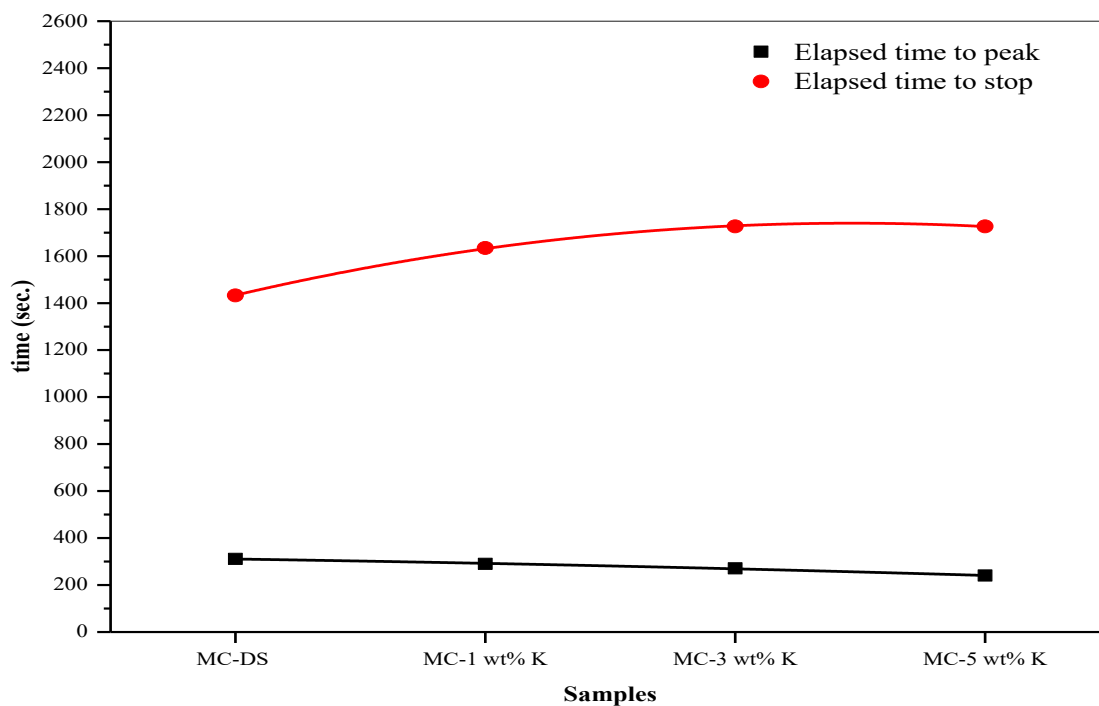


Figure 4-18: Elapsed time for cyclohexane desorption from MC-DS with different amounts of kerogen.

Table 4-8: Residual cyclohexane in MC-DS with different kerogen contents.

sample	volume (μL)	mass (mg)	ppm
MC-DS	0.514	0.40	80
MC-1 wt% K	0.716	0.56	111
MC-3 wt% K	0.123	0.96	191
MC-5 wt% K	0.145	1.13	226

4.4 Effect of kerogen content on the particle sedimentation

4.4.1 Behavior of different fractions of MC-DS in different media

To study the settling behavior of various particles in different solutions, a KRÜSS K100 tensiometer, with capability to use as a sedimentation balance, was used. In this method, a

probe at a fixed location from the liquid surface collected settling particles. In this study, the probe is set to immerse 2 cm in the solvent and the top of the probe is at the middle of the beaker. As Figure 4-19 shows, at the end of sedimentation process the bottom of the probe is just above sedimentation bed. This position is the lowest position for probe in the sedimentation media without interfering of sedimentation bed and the probe. The measurement probe was connected to a sensitive balance that recorded weight changes over time. Most of the weight gain is recorded in short times after experiments start and sedimentation rates slow down by time. Presenting mass-time graphs in logarithmic scales helps to show the changes better at start.

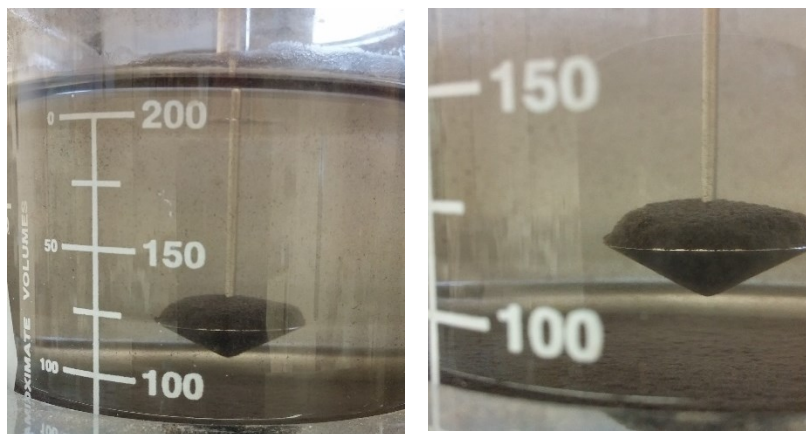


Figure 4-19: position of the probe in sedimentation balance.

Figure 4-20 shows two samples of MC-DS after 30 min of sedimentation in water and cyclohexane. After 30 min in cyclohexane, almost all of fine particles are settled down and the solvent is clear, but in water, fine particles are not settled and makes the water completely opaque.

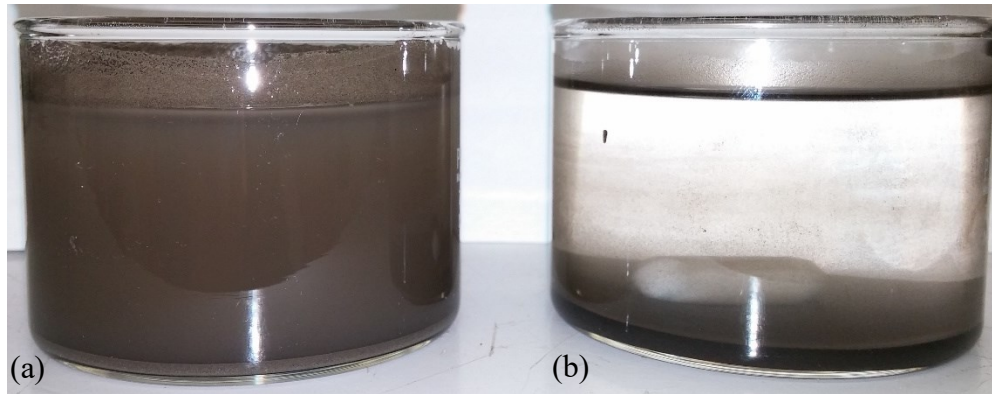


Figure 4-20: MC-DS after 30 min sedimentation. (a) In water, (b) in cyclohexane.

As presented in Figure 4-21, in both liquids, three different stages of sedimentation were observed. The first stage is rapid sedimentation at a constant rate, which finally approaches to another stage with a lower constant rate of sedimentation. There is a transition stage between these two linear stages with non-linear sedimentation behavior. To detect the points that sedimentation behavior changes from almost linear in the 1st stage to non-linear in the 2nd stage and back to linear in the 3rd stage, we need to find the change points in data obtained from sedimentation balance. The change point in our data sets is a time instant at which weight gain of sedimentation balance changes abruptly. *MATLAB* used for data analysis in this part of the study by utilizing “findchangepts” function. This function chooses a random point of data set and divides the signal into two sections. In each section, an empirical estimate of the weight gain is computed and the deviation from this estimate is calculated. Total residual error is calculated section-to-section by adding these deviations. Then the location of the division point optimized to attain the minimum total residual error.

Sedimentation in cyclohexane (Figure 4-21) starts at a high rate and after a short time (on the order of 1 min) more than 95% of the particles are settled and the 3rd stage starts with a low rate. Conversely, sedimentation in water starts at a lower rate than sedimentation in cyclohexane and after a longer time (on the order of 20 min) the 3rd stage with a linear sedimentation rate starts. The total amount of settled particles before the last stage is around 90% and the rest of the sedimentation takes considerable time, which is well documented in the oil sands tailings literature as a problem for oil sands extraction with hot water. Table 4-9 summarizes the sedimentation rates for MC-DS in water and cyclohexane. The sedimentation rate of MC-DS in cyclohexane in the 1st stage is 50% faster than that in water. The sedimentation behavior in water is typical for all fractions of MC-DS, including a low sedimentation rate in the 1st stage and longer time in the 2nd stage of regime change, to approach to a constant rate in the 3rd stage. As such, sedimentation requires a significant amount of time for completion.

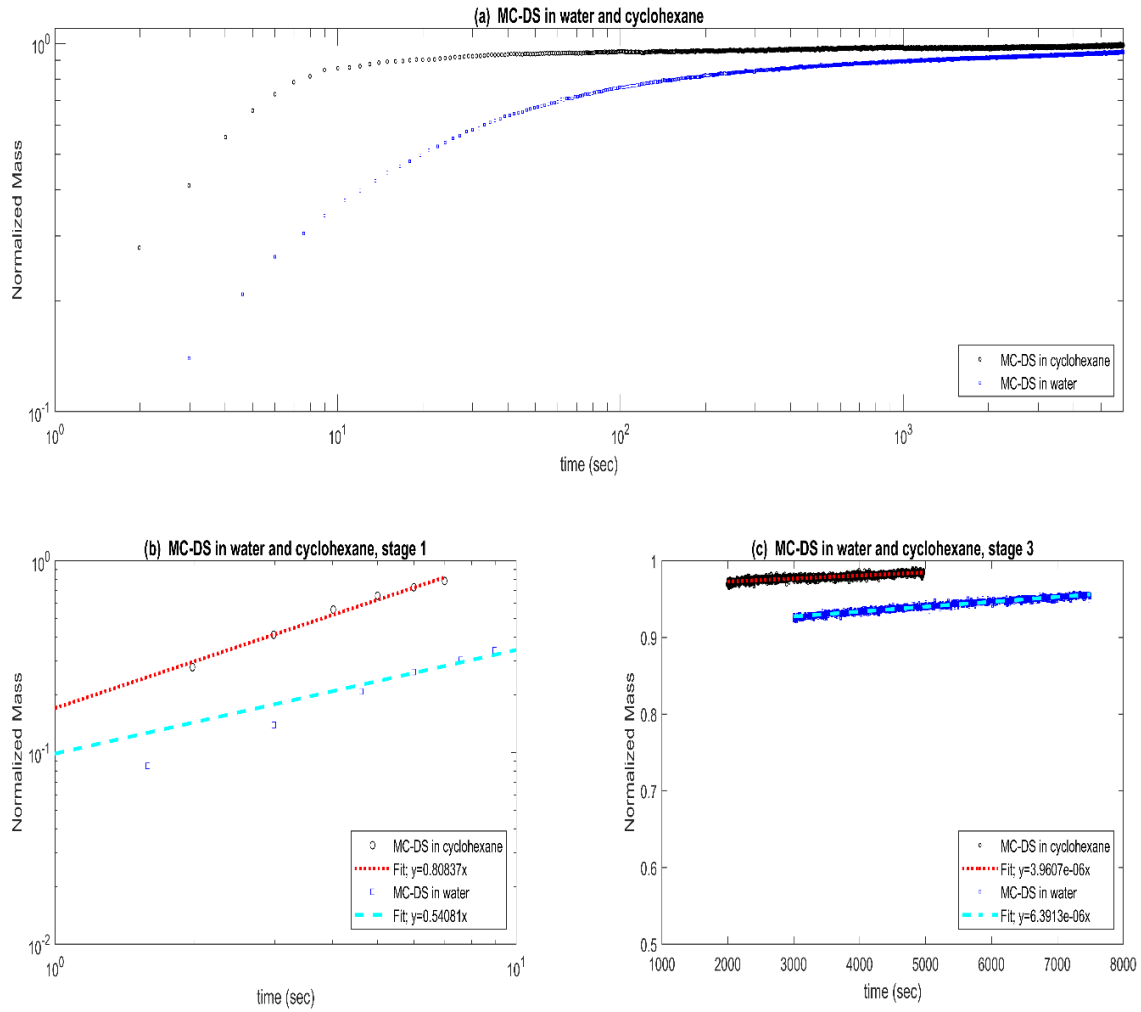


Figure 4-21: Sedimentation behavior of MC-DS in water and cyclohexane, measured by a sedimentation balance. (a) Sedimentation in full scale, (b) closer view of stage one, (c) closer view of stage three.

Table 4-9: Sedimentation rates of 1st and 3rd stages for MC-DS in water and cyclohexane.

Sample	1 st stage rate	3 rd stage rate
MC-DS in water	0.54	6.39E-06
MC-DS in cyclohexane	0.81	3.96E-06

Figure 4-22 shows the sedimentation behavior for MC-DS and its hydrophilic and hydrophobic fractions, MC-L and MC-B, respectively. The 1st stage of sedimentation for MC-L shows a higher rate of 0.83, compared to 0.67 and 0.62 for MC-DS and MC-B, respectively. Faster sedimentation of MC-L can be attributed to its larger particle size distribution than MC-B and MC-DS. MC-DS and its fractions have similar behavior in cyclohexane and there is no significant drop in the sedimentation rates due to contribution from the hydrophobicity of the particles.

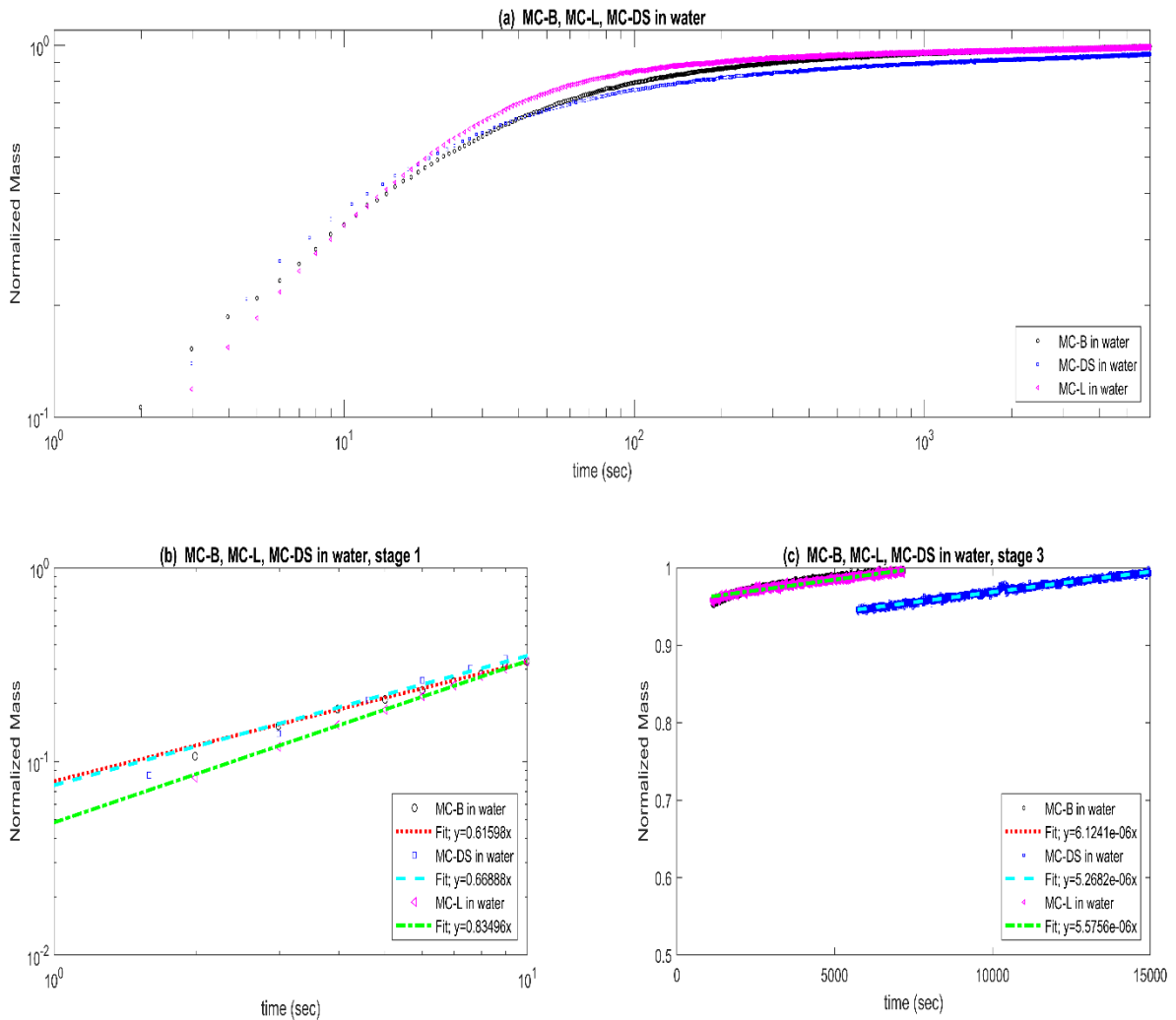


Figure 4-22: Sedimentation behavior of MC-DS and its fractions, MC-B and MC-L, in water, showing the effect of particle characteristics on the 1st and 3rd stages of sedimentation as reflected in the graph slope equations. (a) Sedimentation in full scale, (b) closer view of stage one, (c) closer view of stage three.

By adding bitumen to the cyclohexane, viscosity of the solution is increased, so the behavior of MC-DS is changed. Sedimentation rates in cyclohexane-bitumen are placed between sedimentation rates in pure cyclohexane and water. Figure 4-23 shows that the two linear stages of the sedimentation in the bitumen-cyclohexane solution has the same trend with a high sedimentation rate at 1st that approaches a lower rate in the 3rd stage of sedimentation. The rates for both linear stages have values between those for water and cyclohexane. Also by increasing bitumen content from 5 to 15 wt% the sedimentation would be slower as presented in Figure 4-24.

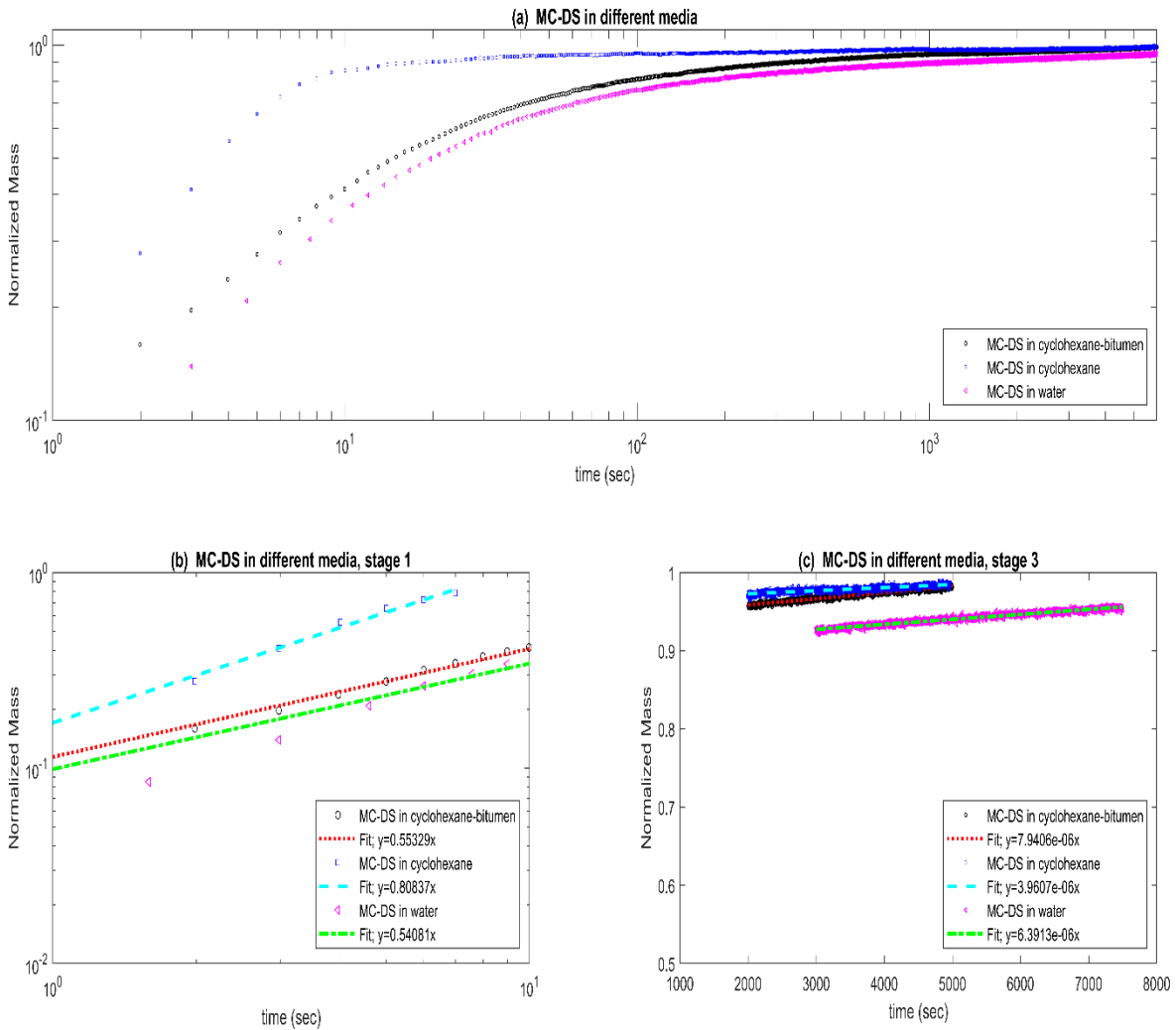


Figure 4-23: Sedimentation of MC-DS in different media, showing the effect of media on the 1st and 3rd stages of sedimentation as reflected in the graph slope equations. (a) Sedimentation in full scale, (b) closer view of stage one, (c) closer view of stage three.

4.4.2 Effect of kerogen content on particle sedimentation

To study the effect of kerogen on the sedimentation of oil sands particles, MC-DS was mixed with 3 and 5 wt% of extracted kerogen in 100 mL of cyclohexane containing 5, 10 and 15 wt% bitumen. The mixtures were sonicated for 1 h, stirred overnight on a hot plate at 50°C and then stored in airtight bags in a vacuum container in a freezer. The sedimentation measurements were executed in cyclohexane with the KRÜSS K100 tensiometer. Samples were immersed in cyclohexane for 1 h with stirring. Figure 4-24 shows the sedimentation of MC-DS with different bitumen contents from 5 to 15 wt% bitumen. After introducing cyclohexane to the samples, bitumen dissolved in the solvent and the viscosity of the sedimentation medium increased. This affected the sedimentation rates, especially in the 1st stage. By increasing the bitumen content in the samples, the 1st stage sedimentation rates were decreased, but the 3rd stages showed similar rates as before. This behavior was repeated for samples with and without kerogen and depended on the bitumen content of the sample. In other words, different kerogen contents in the marine clay samples did not affect the sedimentation rates of the 1st and the 3rd stages, as illustrated in Figure 4-25, Figure 4-26 and Figure 4-27. However, the area in which the sedimentation regime changes from rapid to slow settling is affected. The regime change area is altered in such a way that the total settled mass of particles is lower for higher kerogen contents at the start of the 3rd stage, but sedimentation continues at a similar constant rate. This behavior could be due to slow sedimentation of hydrophobic and fine particles of kerogen in the solvent. The same behavior was observed for different bitumen contents. Table 4-10 listed the rates of the 1st and the 3rd stages of sedimentation in all samples with different kerogen and bitumen contents.

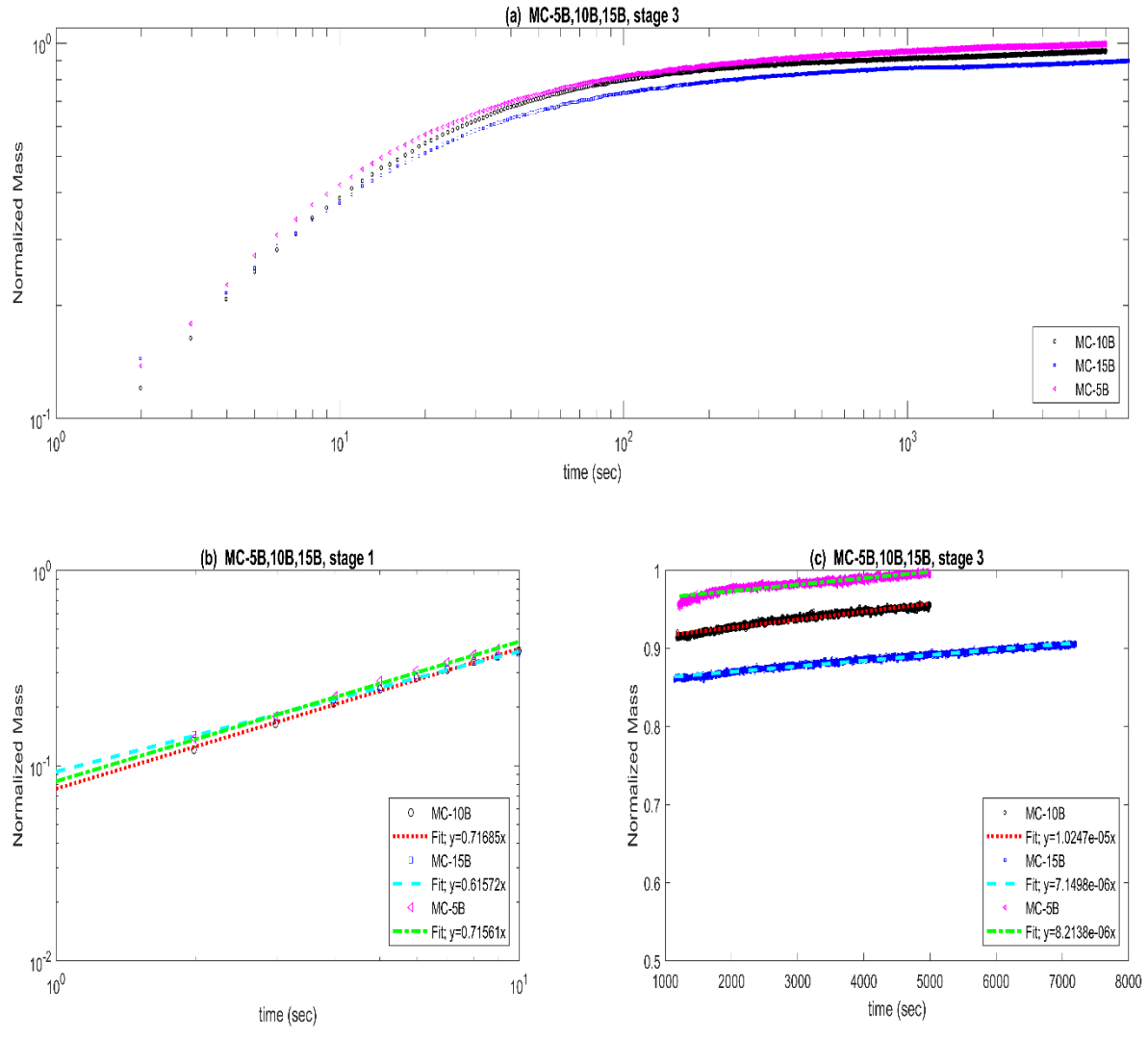


Figure 4-24: Sedimentation behavior of MC with different bitumen contents in cyclohexane, showing the effect of bitumen content on the 1st and 3rd stages of sedimentation as reflected in the graph slope equations.
(a) Sedimentation in full scale, (b) closer view of stage one, (c) closer view of stage three.

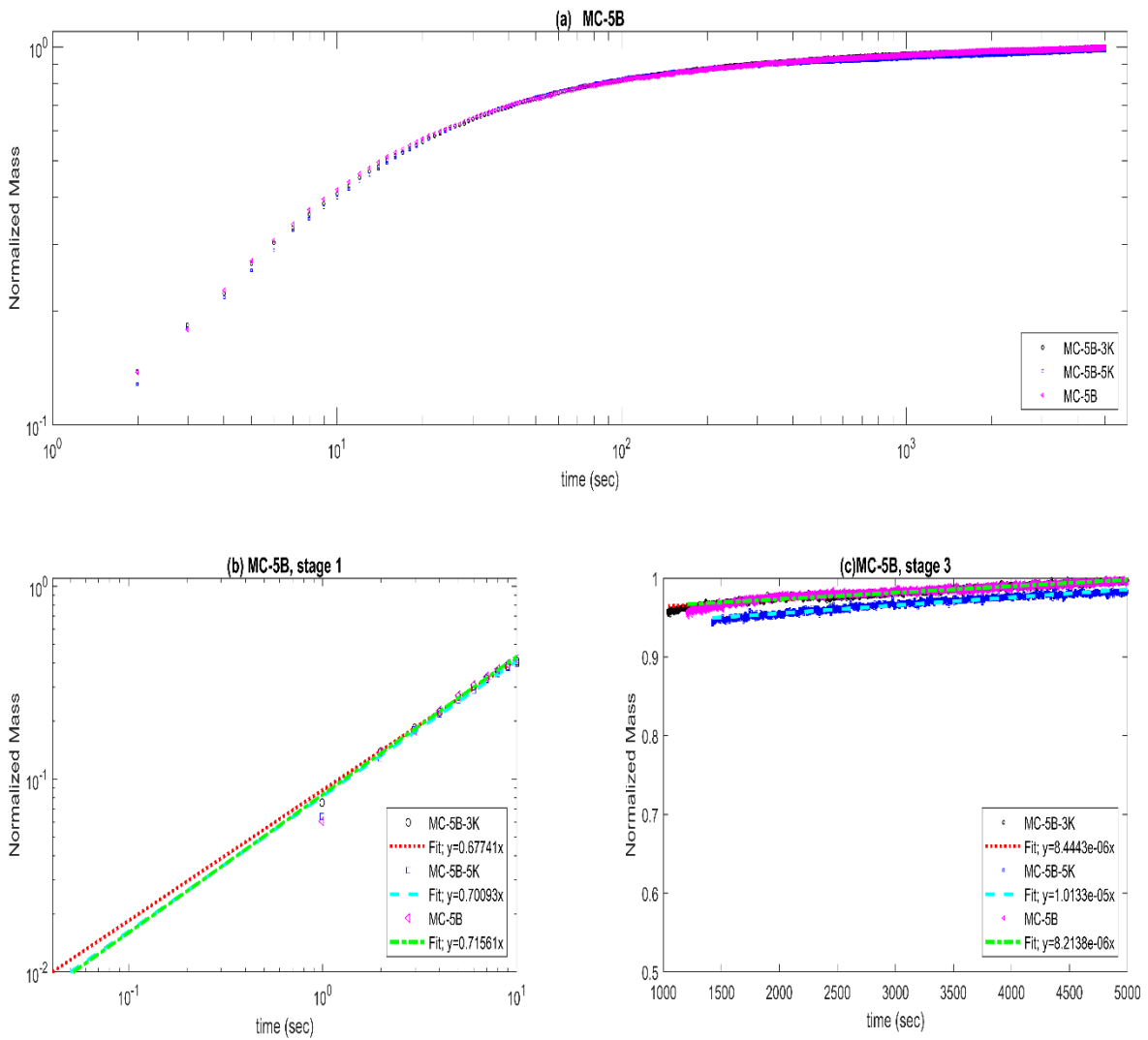


Figure 4-25: Sedimentation of MC-5 wt% bitumen without kerogen and with 3 and 5wt% kerogen in cyclohexane. (a) Sedimentation in full scale, (b) closer view of stage one, (c) closer view of stage three.

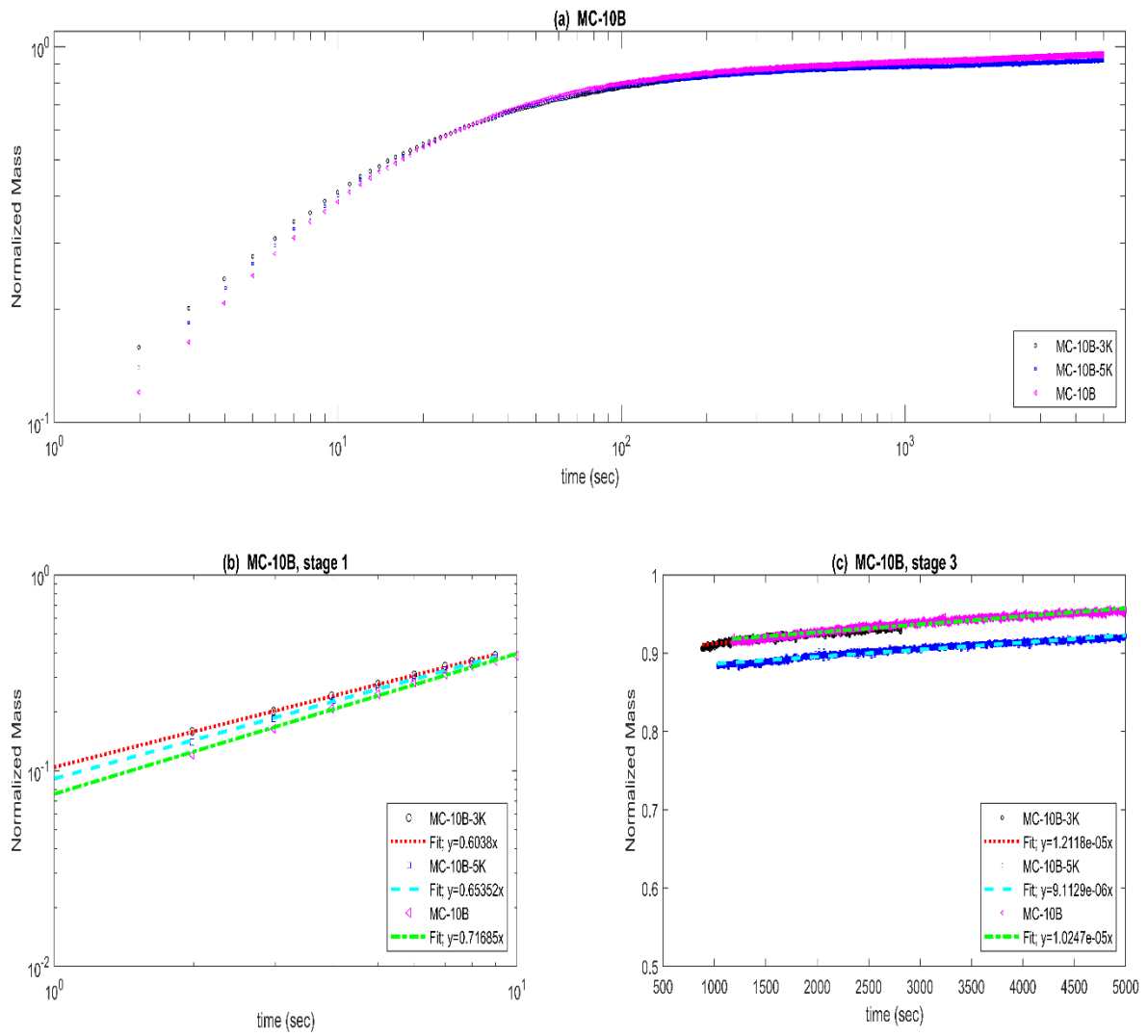


Figure 4-26: Sedimentation of MC-10 wt% bitumen without kerogen and with 3 and 5wt% kerogen in cyclohexane. (a) Sedimentation in full scale, (b) closer view of stage one, (c) closer view of stage three.

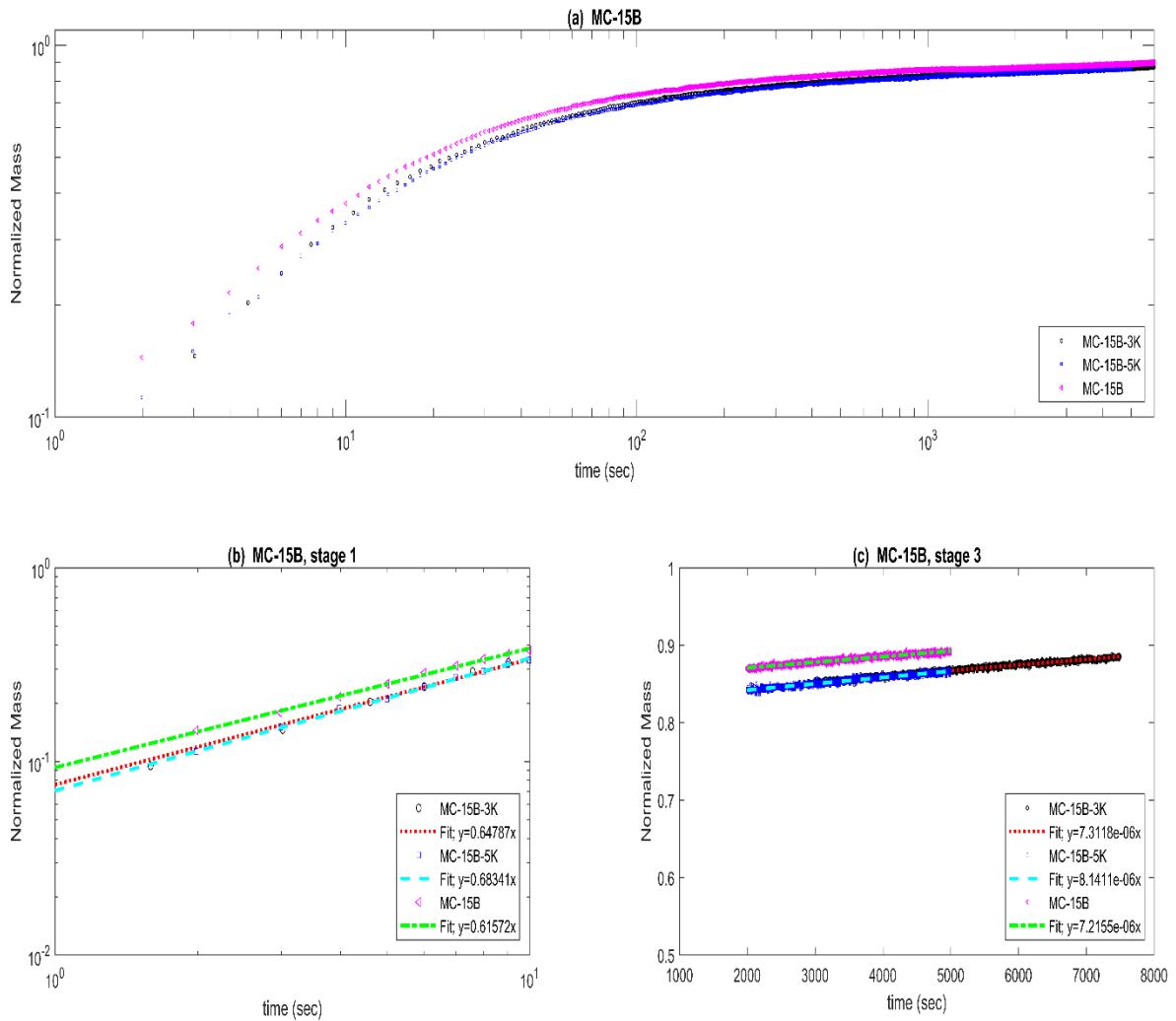


Figure 4-27: Sedimentation of MC-15 wt% bitumen without kerogen and with 3 and 5wt% kerogen in cyclohexane. (a) Sedimentation in full scale, (b) closer view of stage one, (c) closer view of stage three.

Table 4-10: Sedimentation rates of linear stages for MC with different bitumen and kerogen contents in cyclohexane.

Sample	1st stage rate (s⁻¹)	3rd stage rate (s⁻¹)
MC-5B	0.71561	8.2138E-06
MC-5B-3K	0.67741	8.4443E-06
MC-5B-5K	0.70093	10.133-06
MC-10B	0.71685	10.247E-06
MC-10B-3K	0.60380	12.118E-06
MC-10B-5K	0.65352	9.1129E-06
MC-15B	0.61572	7.2155E-06
MC-15B-3K	0.64787	7.3118E-06
MC-15B-5K	0.68341	8.1411E-06

5 Conclusions and future work

5.1 Summary and conclusions

1. Oil sands ores from the North Mine and Aurora Mine of Syncrude Canada Ltd. (Fort McMurray, Alberta) were collected and designated as MC (marine clay), MS (marine sand), EC (estuarine clay) and ES (estuarine sand). These four petrologic end members of estuarine and marine origin were manually homogenized, disaggregated and passed through a sieve with an aperture size of 6.35 mm and then stored frozen in sealed containers in a freezer before use.
2. Dean-Stark extraction was performed to determine the bitumen, solids and water contents of the bulk petrologic end members. The extracted bitumen was stored in a vacuum container in a freezer for further use. Bitumen free solids were dried at 60°C for 24 h, ground gently to disaggregate the possible lumps and stored in airtight containers for further use and characterization.
3. Total organic carbon (TOC) of all end members was measured by CHNS elemental analysis after HCl treatment of bitumen free solids after Dean-Stark extraction. The highest TOC were present in the marine clays. The Aurora Mine marine clay was chosen for kerogen extraction due to its highest TOC. The nitrogen to carbon (N/C) ratio of the marine clay measured by CHNS analysis was 0.021. This N/C ratio was almost two times the corresponding value for extracted bitumen from the same marine clay.
4. A novel fractioning process in water/cyclohexane was performed on marine clay from the Aurora Mine to separate hydrophobic and hydrophilic fractions of the samples. CHNS analysis after HCl treatment revealed that all the organic carbon accumulated

- in the hydrophobic fraction. Based on this finding, only the hydrophobic fraction of the marine clay (MC-B) was treated with acid to extract the kerogen.
5. HCl treatment of the MC-B was performed at room temperature to remove the carbonates and clays. In order to remove the silicates effectively, HCl treated solids were dried at 105°C and treated with HCl-HF at an elevated temperature of 90°C and kept at 60°C for two days. EDX and XRD analysis showed that carbonates, clays and silicates were removed, but some new fluorides were formed during the acid treatment.
 6. To purify the kerogen and eliminate the remaining silicates and newly formed fluorides, the top fraction of kerogen (K-top) was collected during gravity sedimentation of the product of acid treatment. The low fraction (K-low) and heavy sediments of this particle fractioning were also collected for further analysis.
 7. The TN/TOC of the pure kerogen was higher than that for all other fractions and their corresponding bitumen. The presence of pyrite, which is a close associate of organics, was demonstrated through SEM microscopy with EDX and XRD analysis.
 8. During sample preparation, kerogen was not transferred to other clay particles and, after grinding with a mortar and sieving, kerogen was not associated with clay particles. This enabled separation of kerogen-rich particles based on their hydrophobicity by utilizing a novel water/cyclohexane partitioning method. Kerogen accumulated in the hydrophobic fraction and the hydrophilic fraction had almost no organic carbon measured by CHNS elemental analysis.
 9. To measure the residual solvent in the oil sands, marine clay, which is the most problematic end member due to its high clay content, was mixed with cyclohexane and dried at room temperature. Mass spectroscopy of the solvent evaporated from

the samples showed that with higher kerogen content in the oil sands, higher amounts of solvent were retained in oil sands end members.

10. In order to understand the effect of kerogen content on the sedimentation behavior of the oil sands, different oil sands samples with various kerogen and bitumen contents were prepared. Sedimentation results obtained from a sedimentation balance showed that the presence of a higher amount of kerogen did not affect the sedimentation rates of the linear stages but altered the regime change region of the sedimentation process between two linear stages. This affected total particle settlement.

5.2 Future work

The effect of kerogen on solvent retention is important economically and environmentally. In this research solvent retention of different kerogen contents of marine clay were studied by using cyclohexane as a successful and promising solvent candidate for non-aqueous bitumen extraction. This solvent retention of kerogen can be studied more by other solvents to observe how kerogen reacts to different solvents and how much it holds them in its structure.

Kerogen and clay association have not been studied yet. To understand the association of kerogen to inorganics, atomic force microscopy (AFM) and a surface force apparatus (SFA) can investigate the attraction and repulsion forces between kerogen and different clays and quartz. This would be very interesting because during the present study kerogen did not migrate to hydrophilic particles even after grinding and mixing of oil sands particles. This shows that even by mechanical forces during grinding and mixing, kerogen has no tendency to attach to all different oil sands particles and instead it has a significant affinity to hydrophobic particles. AFM and SFA are powerful instruments to study the attraction and repulsion forces between different particles in various media, which can be used to determine kerogen tendency to other particles.

6 References

1. Alberta energy regulator; executive summary data. Retrieved from <https://www.aer.ca/providing-information/data-and-reports/statistical-reports/st98/executive-summary/data.html>, July, 2020.
2. *ST98: Alberta energy outlook, an executive summary*. Published in 2020, Retrieved from <http://www1.aer.ca/st98/2020/data/executive-summary/ST98-2020-Executive-Summary.pdf>, July 2020.
3. Kasperski KL. *Review of research on aqueous extraction of bitumen from mined oil sands; conrad extraction TPG, Calgary, AB (Canada); federal panel on energy research and development, Ottawa, ON (Canada)*. Published in 2001, Canada, Natural Resources Canada. CANMET Western Research Centre, Devon, AB (Canada).
4. Liu J, Xu Z, Masliyah J. Role of fine clays in bitumen extraction from oil sands. *AIChE J.* 2004; 50(8):1917-1927.
5. Mikula RJ, Munoz VA, Wang N, et al. Characterization of bitumen properties using microscopy and near infrared spectroscopy: Processability of oxidized or degraded ores. *J Can Pet Technol.* 2003; 42(08):5.
6. *State of fluid tailings management for mineable oil sands, 2018*. Published in 2019, Retrieved from <https://www.aer.ca/documents/oilsands/2018-State-Fluid-Tailings-Management-Mineable-OilSands.pdf>, July 2020, Alberta Energy Regulator.

7. Alberta government - oil sands information portal. Retrieved from <http://osip.alberta.ca/library/Dataset/Details/542>, July, 2020.
8. *Lower Athabasca region - tailing management framework for the mineable Athabasca oil sands*. Published in 2015, Retrieved from <https://open.alberta.ca/dataset/962bc8f4-3924-46ce-baf8-d6b7a26467ae/resource/7c49eb63-751b-49fd-b746-87d5edee3131/download/2015-larp-tailingsmgtathabascaoilsands.pdf>, July 2020.
9. Alberta oil sands reserves data. Retrieved from <https://www.aer.ca/providing-information/data-and-reports/statistical-reports/st98/reserves.html>, July, 2020.
10. Oil sands area assessment. Retrieved from <https://www.aer.ca/providing-information/data-and-reports/statistical-reports/st98/reserves/oil-sands-area-assessment.html>, July, 2020.
11. Camp FW. *The tar sands of Alberta, Canada*. 3rd ed. Denver: Cameron Engineers; 1976.
12. Kaminsky HAW. *Characterization of an Athabasca oil sands ore and process streams*. [Ph.D.]. University of Alberta (Canada); 2008.
13. Hooshier Fard MA. *Characterization of clay minerals in the Athabasca oil sands in water extraction and non-aqueous solvent extraction processes*. [Ph.D.]. University of Alberta (Canada); 2011.

14. Masliyah JH, Xu Z, Czarnecki JA, Dabros M. *Handbook on theory and practice of bitumen recovery from athabasca oil sands*. Cochrane, Alta.: Kingsley Knowledge Pub.; 2011.
15. Liu J, Xu Z, Masliyah J. Interaction forces in bitumen extraction from oil sands. (report). *J Colloid Interface Sci*. 2005(2):507.
16. Chalaturnyk RJ, Scott JD, Ozum B. Management of oil sands tailings. *Petrol Sci Technol*. 2002; 20(9):1025-1046.
17. SrinivasaRajagopalan S. *Study of bitumen liberation from oil sands ores*. [M.Sc.]. University of Alberta (Canada); 2010.
18. Masliyah J, Zhou ZJ, Xu ZH, Czarnecki J, Hamza H. Understanding water-based bitumen extraction from athabasca oil sands. *Can J Chem Eng*. 2004; 82(4):628-654.
19. Muñoz VA, Kasperski KL, Omotoso OE, Mikula RJ. The use of microscopic bitumen froth morphology for the identification of problem oil sand ores. *Petrol Sci Technol*. 2003; 21(9-10):1509-1529.
20. Nikakhtari H, Vagi L, Choi P, Liu Q, Gray MR. Solvent screening for non-aqueous extraction of alberta oil sands. *Can J Chem Eng*. 2013; 91(6):1153-1160.
21. Hooshar A, Uhlik P, Liu Q, Etsell TH, Ivey DG. Clay minerals in non-aqueous extraction of bitumen from Alberta oil sands part 1. Non-aqueous extraction procedure. *Fuel Process Technol*. 2012; 94(1):80-85.

22. Hooshlar A, Uhlík P, Ivey DG, Liu Q, Etsell TH. Clay minerals in non-aqueous extraction of bitumen from Alberta oil sands. part 2. Characterization of clay minerals. *Fuel Process Technol.* 2012; 96:183-194.
23. Hooshlar A, Uhlík P, Kaminsky HW, et al. High resolution transmission electron microscopy study of clay mineral particles from streams of simulated water based bitumen extraction of Athabasca oil sands. *Appl Clay Sci.* 2010; 48(3):466-474.
24. Kaminsky HAW, Etsell TH, Ivey DG, Omotoso O. Distribution of clay minerals in the process streams produced by the extraction of bitumen from Athabasca oil sands. *The Canadian Journal of Chemical Engineering.* 2009; 87(1):85-93.
25. Eslahpazir R, Kupsta M, Liu Q, Ivey DG. Sample preparation method for characterization of fine solids in Athabasca oil sands by electron microscopy. *Energy Fuels.* 2011; 25(11):5158-5164.
26. Kotlyar LS, Kodama H, Sparks BD, Grattan-Bellew PE. Non-crystalline inorganic matter-humic complexes in Athabasca oil sand and their relationship to bitumen recovery. *Appl Clay Sci.* 1987; 2(3):253-271.
27. Eslahpazir R, Liu Q, Ivey DG. Characterization of iron-bearing particles in Athabasca oil sands. *Energy Fuels.* 2012; 26(8):5036-5047.
28. Osacky M, Geramian M, Dyar MD, et al. Characterisation of petrologic end members of oil sands from the Athabasca region, Alberta, Canada. *The Canadian Journal of Chemical Engineering.* 2013; 91(8):1402-15.

29. Ignasiak TM, Kotlyar L, Longstaffe FJ, Strausz OP, Montgomery DS. Separation and characterization of clay from Athabasca asphaltene. *Fuel*. 1983; 62(3):353-362.
30. Mercier PHJ, Patarachao B, Kung J, et al. X-ray diffraction (XRD)-derived processability markers for oil sands based on clay mineralogy and crystallite thickness distributions. *Energy Fuels*. 2008; 22(5):3174-3193.
31. Omotoso OE, Mikula RJ. High surface areas caused by smectitic interstratification of kaolinite and illite in Athabasca oil sands. *Appl Clay Sci*. 2004;25(1):37-47.
32. Bayliss P, Levinson AA. *Mineralogical review of the Alberta oil sand deposits (lower cretaceous, manville group)*. Vol 24. ; 1976:211-224.
33. Bichard JA. *Oil sands composition and behaviour research. The research papers of John A. bichard 1957-1965*. Published in 1987, Edmonton, AB, Alberta Oil Sands Technology and Research Authority.
34. Spiers GA, Dudas MJ, Turchenek LW. The chemical and mineralogical composition of soil parent materials in northeast alberta. *Can J Soil Sci*. 1989; 69(4):721-737.
35. Sparks BD, Kotlyar LS, O'Carroll JB, Chung KH. Athabasca oil sands: Effect of organic coated solids on bitumen recovery and quality. *Journal of Petroleum Science and Engineering; Reservoir Wettability*. 2003; 39(3):417-430.

36. Osacky M, Geramian M, Ivey DG, Liu Q, Etsell TH. Mineralogical and chemical composition of petrologic end members of Alberta oil sands. *Fuel*. 2013; 113(0):148-157.

37. Wallace D, Tipman R, Komishke B, Wallwork V, Perkins E. Fines/water interactions and consequences of the presence of degraded illite on oil sands extractability. *Can J Chem Eng*. 2004; 82(4):667-677.

38. Wang C, Geramian M, Liu Q, Ivey DG, Etsell TH. Comparison of different methods to determine the surface wettability of fine solids isolated from Alberta oil sands. *Energy Fuels*. 2015; 29(6):3556-3565.

39. Hein FJ, Marsh RA, Boddy MJ. Overview of the oil sands and carbonate bitumen of Alberta: Regional geologic framework and influence of salt-dissolution effects. *AAPG Hedberg Conference, "Heavy Oil and Bitumen in Foreland Basins – From Processes to Products"*. 2008.

40. Hans GM, Mary LB, Eugene D, Harald H, Luo P, Yi Z. The grosmont: A complex dolomitized, fractured and karstified heavy oil reservoir in a devonian carbonate-evaporite platform. *GeoConvention 2012 vis 2012*; 10576:1–24. .

41. Rossenfoss S. Finding pathways to produce heavy oil from Canadian carbonates. *J pet technol* 2013.

42. Procter RM, Taylor GC, Wade J. Oil and natural gas resources of Canada 1983. *inst sediment pet geol* 1984:59.

43. Hepler LG, Hsi C, Alberta Oil Sands Technology and Research Authority. *AOSTRA technical handbook on oil sands, bitumens and heavy oils*. Alberta Oil Sands Technology and Research Authority; 1989.
44. Couillard M, Mercier PHJ. Analytical electron microscopy of carbon-rich mineral aggregates in solvent-diluted bitumen products from mined Alberta oil sands. *Energy Fuels*. 2016; 30(7):5513-5524.
45. Ellwood BB, Burkart B, Rajeshwar K, et al. Are the iron carbonate minerals, ankerite and ferroan dolomite, like siderite, important in paleomagnetism? *J Geophys Res*. 1989; 94:7321-7331.
46. Wills BA, Finch J. *Wills' mineral processing technology: An introduction to the practical aspects of ore treatment and mineral recovery*. Butterworth-Heinemann; 2015.
47. Omotoso O, Munoz VA, Mikula RJ. Valuable minerals in the UTS fort hill oil sands lease core samples; 2005.
48. Moore DM, Reynolds RC. *X-ray diffraction and the identification and analysis of clay minerals*. 2nd Ed. New York: Oxford University Press; 1997.
49. Bergaya F, Theng BKG, Lagaly G. *Handbook of clay science*. Vol 1. Amsterdam; London: Elsevier; 2006.
50. Moore DM, Hower J. Ordered interstratification of dehydrated and hydrated nanosmectite. *Clays Clay Miner*. 1986; 34(4):379-384.

51. Clementz DM. Interaction of petroleum heavy ends with montmorillonite. *clay and clay minerals*. 1976; 24(6):312-19.
52. Dongbao F, Woods JR, Kung J, et al. Residual organic matter associated with toluene-extracted oil sands solids and its potential role in bitumen recovery via adsorption onto clay minerals . *Energy Fuels*. 2010; 24(4):2249-2256.
53. Wallace D, Tipman R, Komishke B, Wallwork V, Perkins E. - Fines/water interactions and consequences of the presence of degraded illite on oil sands extractability. *The Canadian Journal of Chemical Engineering*. 2004; 82(4):667-677.
54. Tu Y, O'Carroll JB, Kotlyar LS, et al. Recovery of bitumen from oil sands: Gelation of ultra-fine clay in the primary separation vessel. *Fuel*. 2005; 84(6):653-660.
55. Brenner H. Rheology of a dilute suspension of axisymmetric brownian particles. *Int J Multiphase Flow*. 1974; 1(2):195-341.
56. Sanford EC. Processibility of Athabasca oil sand: Interrelationship between oil sand fine solids, process aids, mechanical energy and oil sand age after mining. *The Canadian Journal of Chemical Engineering*. 1983; 61(4):554-567.
57. Chong J, Ng S, Chung KH, Sparks BD, Kotlyar LS. Impact of fines content on a warm slurry extraction process using model oil sands. *Fuel*. 2003; 82(4):425-438.
58. Mercier PHJ, Le Page Y, Tu Y, Kotlyar L. Powder X-ray diffraction determination of phyllosilicate mass and area versus particle thickness distributions for clays from the Athabasca oil sands. *Petrol Sci Technol*. 2008; 26(3):307-321.

59. Mercier PHJ, Ng S, Moran K, et al. Colloidal clay gelation: Relevance to current oil sands operations. *Petrol Sci Technol*. 2012; 30(9):915-923.
60. Tissot BP, Welte DH. Geochemical fossils and their significance in petroleum formation. In: *Petroleum formation and occurrence*. Springer; 1984:93-130.
61. Strausz O, Lown EM. *The chemistry of Alberta oil sands, bitumens and heavy oil*. Canada: Alberta Energy Research Inst., Calgary, AB (Canada); 2003.
62. Odebunmi EO, Olaremu AG. Extraction of chemical constituents of bitumen using a mixed solvent system. *Open Journal of Applied Sciences*. 2015; 5(08):485.
63. Vandenbroucke M. Kerogen: From types to models of chemical structure. *Oil & Gas Science and Technology - Rev.IFP*. 2003; 58(2):243-269.
64. Vandenbroucke M, Largeau C. Review: Kerogen origin, evolution and structure. *Org Geochem*. 2007; 38:719-833.
65. Adams JJ, Rostron BJ, Mendoza CA. Coupled fluid flow, heat and mass transport, and erosion in the Alberta basin; implications for the origin of the Athabasca oil sands. *Canadian Journal of Earth Sciences*. 2004; 41(9; 9):1077-1095.
66. Peters KE, Moldowan JM. *The biomarker guide; interpreting molecular fossils in petroleum and ancient sediments*. United States: Prentice Hall: Englewood Cliffs, NJ, United States; 1993.

67. Zheng L. *Characterization of clay minerals and kerogen in Alberta oil sands geological end members*. [M.Sc.]. University of Alberta (Canada); 2013.
68. Boyer C, Kieschnick J, Suarez-Rivera R, Lewis RE, Waters G. Producing gas from its source. *Oilfield Review*. 2006; 18(3; 3):36-49.
69. Glorioso JC, Rattia A. *Unconventional reservoirs: Basic petrophysical concepts for shale gas*. 2012.
70. Cornelissen G, Gustafsson O, Bucheli TD, Jonker MTO, Koelmans AA, van Noort, Paul C. M. Extensive sorption of organic compounds to black carbon, coal, and kerogen in sediments and soils; mechanisms and consequences for distribution, bioaccumulation, and biodegradation. *Environmental Science & Technology, ES & T*. 2005; 39(18; 18):6881-6895.
71. Geramian M, Ivey DG, Liu Q, Etsell TH. Characterization of four petrologic end members from Alberta oil sands and comparison between different mines and sampling times. *Can J Chem Eng*. 2018; 96(1):49-61.
72. Panda S. *Role of residual bitumen on the solvent removal from Alberta oil sands gangue*. [M.Sc.] University of Alberta (Canada); 2016.
73. Ejike LI. *Role of fine solids in solvent recovery from reconstituted Alberta oil sands gangue*. [M.Sc.] University of Alberta (Canada); 2016.
74. Khalkhali R. *Role of the composition of cyclohexane-extracted gangue on its drying at ambient conditions*. [M.Sc.] University of Alberta (Canada); 2020.